Combining tower mixing ratio and community model data to estimate regional-scale net ecosystem carbon exchange by boundary layer inversion over four flux towers in the United States

Xuerui Dang,[1,2] Chun-Ta Lai,[2] David Y. Hollinger,[3] Andrew J. Schauer,[4] Jingfeng Xiao,[5] J. William Munger,[6] Clenton Owensby,[7] and James R. Ehleringer[8]

[1]   We evaluated an idealized boundary layer (BL) model with simple parameterizations using vertical transport information from community model outputs (NCAR/NCEP Reanalysis and ECMWF Interim Analysis) to estimate regional-scale net CO_2 fluxes from 2002 to 2007 at three forest and one grassland flux sites in the United States. The BL modeling approach builds on a mixed-layer model to infer monthly average net CO_2 fluxes using high-precision mixing ratio measurements taken on flux towers. We compared BL model net ecosystem exchange (NEE) with estimates from two independent approaches. First, we compared modeled NEE with tower eddy covariance measurements. The second approach (EC-MOD) was a data-driven method that upscaled EC fluxes from towers to regions using MODIS data streams. Comparisons between modeled CO_2 and tower NEE fluxes showed that modeled regional CO_2 fluxes displayed interannual and intra-annual variations similar to the tower NEE fluxes at the Rannells Prairie and Wind River Forest sites, but model predictions were frequently different from NEE observations at the Harvard Forest and Howland Forest sites. At the Howland Forest site, modeled CO_2 fluxes showed a lag in the onset of growing season uptake by 2 months behind that of tower measurements. At the Harvard Forest site, modeled CO_2 fluxes agreed with the timing of growing season uptake but underestimated the magnitude of observed NEE seasonal fluctuation. This modeling inconsistency among sites can be partially attributed to the likely misrepresentation of atmospheric transport and/or CO_2 gradients between ABL and the free troposphere in the idealized BL model. EC-MOD fluxes showed that spatial heterogeneity in land use and cover very likely explained the majority of the data-model inconsistency. We show a site-dependent atmospheric rectifier effect that appears to have had the largest impact on ABL CO_2 inversion in the North American Great Plains. We conclude that a systematic BL modeling approach provided new insights when employed in multiyear, cross-site synthesis studies. These results can be used to develop diagnostic upscaling tools, improving our understanding of the seasonal and interannual variability of surface CO_2 fluxes.

1.   Introduction

[2]   Estimating the net carbon balance of terrestrial eco-systems requires a strategy that integrates observations and modeling methods. This is because no single model or mea-surement approach can sufficiently provide the large amount

[1]College of Forestry, Northwest A&F University, Shaanxi, China.

[2]Department of Biology, San Diego State University, San Diego, California, USA.

[3]Northern Research Station, USDA Forest Service, Durham, New Hampshire, USA.

[4]Department of Earth and Space Sciences, University of Washington, Seattle, Washington, USA.

[5]Complex Systems Research Center, Institute for the Study of Earth, Oceans, and Space, University of New Hampshire, Durham, New Hampshire, USA.

[6]School of Engineering and Applied Science and Department of Earth and Planetary Science, Harvard University, Cambridge, Massachusetts, USA.

[7]Department of Agronomy, Kansas State University, Manhattan, Kansas, USA.

[8]Department of Biology, University of Utah, Salt Lake City, Utah, USA.

of information required to explain the considerable interannual variation in the capacity of land carbon sinks [*Le Quéré et al.*, 2009]. The need for a systematic model-data fusion approach and error analyses to quantify terrestrial carbon balance has been previously emphasized [*Raupach et al.*, 2005; *Wang et al.*, 2009]. Following the model-data fusion concept, recent studies have combined statistical/modeling techniques, remotely sensed data products, and climate data to upscale tower-based flux measurements to a region [*Chen et al.*, 2008; *Running et al.*, 2004; *Xiao et al.*, 2008, 2010, 2011]. However, interpretation of remote sensing-based model results remains at times difficult and uncertain because of their coarse resolution and scale mismatch when compared to tower eddy covariance fluxes [*Dolman et al.*, 2009; *Gamon et al.*, 2006a; *Mahrt*, 1998].

[3] Another commonly used approach related to the model-data fusion concept is the atmospheric inversion technique. Global atmospheric inversion analyses utilize precise concentration data obtained from flask networks [*Conway et al.*, 1994; *Keeling et al.*, 1996, 2011; *Tans et al.*, 1990], combined with a priori knowledge of atmospheric transport, to infer global distributions of carbon sources and sinks [*Battle et al.*, 2000; *Ciais and Meijer*, 1998; *Enting et al.*, 1995; *Fan et al.*, 1998; *Gurney et al.*, 2002; *Keeling et al.*, 1996, 2011; *Peters et al.*, 2007; *Rayner and O'Brien*, 2001]. These global analyses provide top-down estimates of land-ocean uptake partitioning of anthropogenic CO$_2$ emissions, but they do not offer sufficient resolution to decipher the variability and controls of subgrid-scale fluxes.

[4] As a result, a great deal of effort has been devoted to developing reliable methods that are capable of quantifying regional carbon budgets. CO$_2$ mixing ratios measured by aircraft [*Desjardins et al.*, 1992; *Dolman et al.*, 2006; *Gatti et al.*, 2010; *Gerbig et al.*, 2003; *Gibert et al.*, 2007; *Gioli et al.*, 2004; *Stephens et al.*, 2007; *Sun et al.*, 2010] or on tall towers [*Bakwin et al.*, 1998; *Desai et al.*, 2010; *Gloor et al.*, 2001; *Helliker et al.*, 2004; *Wang et al.*, 2007; *Yi et al.*, 2004] may be used to infer regional surface fluxes on land. However, applying atmospheric inversion techniques regionally has been more challenging because conservation of momentum is rarely met in the model at this spatial scale. The evolution of the atmospheric boundary layer (ABL) is influenced by synoptic weather patterns [*Hurwitz et al.*, 2004] and the complex interaction between entrainment, subsidence, topography, cloud effects, and horizontal advection [*Stull*, 1988]. This complexity means that the momentum fluxes cannot be easily conserved using simplifications such as zero divergence on diurnal timescales, in which the daytime BL is often unstable and nocturnal BL is strongly stable. Nevertheless, attempts to infer surface fluxes from mixing ratio data are highly dependent on the atmospheric transport. ABL studies estimating diurnal CO$_2$ exchange over land [*Chen et al.*, 2008; *Denmead et al.*, 1996; *Gerbig et al.*, 2003; *Gibert et al.*, 2007; *Gloor et al.*, 2001; *Larson and Volkmer*, 2008; *Levy et al.*, 1999; *Lloyd et al.*, 2001; *Moore and Fitzjarrald*, 1993; *Styles et al.*, 2002; *Wofsy et al.*, 1988] have reported widely variable agreement when compared to bottom-up approaches [*Desai et al.*, 2010; *Fitzjarrald*, 2004].

[5] Surface CO$_2$ and H$_2$O fluxes and the ABL dynamics are commonly driven by solar radiation, which leads to strong covariance between the variations in the ABL depth and net CO$_2$ fluxes (the rectifier effect [*Denning et al.*, 1996]). This is an interesting phenomenon that has not been adequately investigated, particularly at the site level near flux towers, except for a handful of studies conducted at the WLEF flux site in Wisconsin, United States [*Denning et al.*, 2008; *Yi et al.*, 2004]. Furthermore, a number of studies applied the equilibrium BL concept to estimate regional CO$_2$ fluxes [*Bakwin et al.*, 2004; *Desai et al.*, 2010; *Helliker et al.*, 2004; *Lai et al.*, 2006a]. Despite the success of this model, an adequate explanation is still lacking for why monthly averages from an idealized BL model are able to produce reasonable agreement when compared to tower NEE measurements. Here we explore these correlations between the ABL CO$_2$ balance and the boundary layer evolution using a BL modeling approach.

[6] Our goal is to evaluate an idealized BL model of simple parameterizations using vertical transport information from the community models (NCAR/NCEP Reanalysis and ECMWF Interim Analysis). We estimated regional-scale net CO$_2$ fluxes from 2002 to 2007 at three forest and one grassland flux sites in the United States. The BL modeling approach builds on a mixed layer model to infer monthly average net CO$_2$ fluxes using high-precision mixing ratio measurements recorded on flux towers. We used CO$_2$ mixing ratios derived from the marine boundary layer [*GLOBALVIEW-CO2*, 2009] as a proxy to represent those in the free troposphere. This proxy was compared to aircraft CO$_2$ observations made at the height 2000–3000 m asl over Harvard Forest where aircraft data were available. We compared BL model NEE with estimates from two independent approaches. First, we compared modeled NEE with tower eddy covariance (EC) measurements. The second approach (EC-MOD) combines EC flux measurements and remote sensing products (MODIS), and has been developed to estimate continental-scale gross primary productivity and net ecosystem exchange (NEE) of CO$_2$ [*Xiao et al.*, 2010, 2011]. The first objective of the present study is to evaluate the applicability of a BL model to regions of differing biomes, land use history and climatic variability by coupling surface CO$_2$ observations with simple parameterizations that are readily available from atmospheric databases (i.e., NCAR Reanalysis, Globalview-CO$_2$ and ECMWF Analysis). Our second objective is to contrast regional flux estimates of the two independent approaches with the tower EC measurements. We performed a suite of sensitivity and error analyses to quantify the uncertainty regarding the BL inversion approach, and discuss merits and limitations associated with each method.

2. Materials and Methods

2.1. Boundary Layer Modeling Approach

[7] Assuming a fully mixed convective boundary layer (CBL), a simple BL budget equation can be written as [*Denmead et al.*, 1996; *McNaughton*, 1989; *Raupach*, 1991]:

$$\frac{dC}{dT} = \frac{F_c}{\rho h} + \left(\frac{C_{FT} + C}{\rho h}\right)\left(\frac{dh}{dt} - W_{FT}\right) \quad (1)$$

where ρ is the density of air and assumed constant in the CBL, h is the CBL depth, and t is time. F_c is the net surface flux of CO$_2$, C represents the well-mixed CO$_2$ mixing ratio in the

CBL, C_{FT} is the CO$_2$ mixing ratio in the free troposphere, and W_{FT} is the mean vertical velocity at the top of CBL. The time derivative in equation (1) is a total derivative that, for the left-hand side, includes a time rate of change term ($\partial C/\partial t$) and mean advection terms ($u\partial C/\partial x$, $v\partial C/\partial y$, $w\partial C/\partial z$). Assuming negligible horizontal and vertical advection [*de Arellano et al.*, 2004], by rearranging equation (1) leads to:

$$\rho h \frac{\partial C}{\partial t} = F_c - \rho\left(W_{FT} - \frac{\partial h}{\partial t}\right)(C_{FT} - C) = F_c - \rho\overline{W}(C_{FT} - C)$$
(2)

where $\overline{W} = W_{FT} - \dfrac{\partial h}{\partial t}$ is the mean entrainment rate, and the overbar represents time averaging over a month.

[8] The assumption of negligible advection that leads to equation (2) is likely violated on daily time scales [*Styles et al.*, 2002]. In this study, we postulate that the mid-afternoon BL approaches a steady state in which the nonlinearity associated with diurnal BL processes are presumably reduced when integrated over monthly time scales. This assumption is supported by direct observations of the CBL CO$_2$ profile by instrumentation on a tall tower in northern Wisconsin, United States [*Yi et al.*, 2000, 2001]. *Yi et al.* [2000, Figure 1] provide evidence suggesting a zero rate of CO$_2$ change (i.e., $\partial C/\partial t = 0$) in the CBL, and *Yi et al.* [2001, Figure 5] lend supports to negligible vertical change (i.e., $\partial h/\partial t = 0$). Assuming these direct observations of CBL phenomena apply, equation (2) can be further simplified to:

$$F_c = \rho\overline{W}(C_{FT} - C)$$
(3)

The term $\rho\overline{W}$ is a flux density (in units of mol *air* m^{-2} s^{-1}). Flux densities were preferred to the use of a true velocity because flux densities were independent of pressure and temperature and were more readily comparable across sites. If velocity were desired, the vertical variation of air density in the ABL would have to be accounted for [*Betts*, 2000; *Betts et al.*, 2004]. We will use flux densities to express mean entrainment rates of air into the ABL from the free troposphere throughout this study.

[9] The assumption that a steady state boundary layer exists when BL processes are integrated over monthly time scales is critical to our regional flux estimates but unfortunately very difficult to directly verify. The idea is similar to the concept of equilibrium ABL budget for water and energy over the tropical ocean proposed by *Betts and Ridgway* [1989]. *Betts* [2000] extended the theory to propose the idealized equilibrium BL concept over land. Briefly stated here, the idealized equilibrium BL model considers a hypothetical steady state mixed layer over land where diurnal averages of mass and energy exchange in the ABL are balanced primarily between surface fluxes, radiation and subsidence. A number of studies evaluated the idealized equilibrium BL approach against scalar measurements, including potential temperature and humidity in large river basins [*Betts*, 2000], CO$_2$ (and water vapor) fluxes in temperature forests [*Bakwin et al.*, 2004; *Betts et al.*, 2004; *Desai et al.*, 2010; *Helliker et al.*, 2004, 2005] and a tallgrass prairie [*Lai et al.*, 2006a]. For the present study, we conduct a suite of sensitivity analyses to quantify errors associated with our simple BL approach.

2.2. Study Sites

[10] Our study uses data from four long-term flux sites in the United States, including Harvard Forest, MA (42.538°N, 72.171°W), Howland Forest, ME (45.204°N, 68.74°W), Wind River Experimental Forest, WA (45.821°N, 121.952°W), and a C$_4$-dominated tallgrass prairie (Rannells Flint Hills prairie near Manhattan, KS, 39.083°N, 96.533°W). These four sites were carefully selected, representing major vegetation types in the AmeriFlux network with different climatic variability. General site information including dominant vegetation species and long-term mean climatic conditions are summarized in Table 1. At all sites, NEE was measured by eddy covariance using standard configurations complying with AmeriFlux guidelines [*Goulden et al.*, 1996; *Hollinger et al.*, 2004; *Lai et al.*, 2006a; *Paw U et al.*, 2004].

[11] Figure 1 shows land classification maps in the vicinity of the three forest sites. These maps were provided by NOAA Coastal Services Center and accessible on its website (http://www.csc.noaa.gov). The corner coordinates are relative to center of pixel and the pixel size is 30 m × 30 m, giving high resolution of land cover. Each map shows a 1° × 1° area (~10^4 km^2) centered on a flux tower, a size approximating the footprint of potential source areas for mixing ratio measurements [*Gloor et al.*, 2001]. The Howland forest flux tower sits at the ecotone between the deciduous northern hardwood forest and subboreal coniferous forest (*Picea rubens* and *Tsuga canadensis*). The area is bound by a mosaic landscape of mixed deciduous and evergreen forests and wetlands. The Harvard Forest flux tower is located in the midst of a mixed hardwood forest that resembles the dominant vegetation type (*Quercus rubra* and *Acer rubrum*) in the region. Major land cover types that potentially contribute to the source areas of trace gas mixing ratio measurements include eastern deciduous forests, developed land areas ranging from medium to high intensity and a large water body (Quabbin Reservoir) roughly 20 km southwest of the site. The Wind River flux tower is located in the midst of a western old growth coniferous forest (dominated by *Pseudotsuga menziesii*) surrounded by relatively uniform vegetation cover but varying stand age. Differences in the complexity of land cover are likely to contribute to interannual variability in the atmospheric CO$_2$ mixing ratios and regional fluxes inferred from the mixing ratio measurements. The Rannells Prairie flux tower is located in the midst of a managed, ungrazed grassland in which productivity is primarily controlled by moisture availability and the seasonal dynamics of C$_3$ (*Carex sp.* and *Vernonia baldwinii*) and C$_4$ (*Andropogon gerardii* and *Sorghastrum nutans*) photosynthesis. The effect of spatial heterogeneity on trace gas mixing ratios, isotopic composition and flux measurements in Rannells Prairie has been reported elsewhere [*Lai et al.*, 2003, 2006a, 2006b].

2.3. Air Sample Collection and Analysis

[12] We measured CO$_2$ mixing ratios in the convective boundary layer by analyzing air samples collected by an automated flask sampler [*Schauer et al.*, 2003] at each of the four study sites following the procedure described by *Lai et al.* [2004, 2005, 2006b]. Briefly, dry air samples were collected at weekly intervals using 100 ml flasks (Kontes

Table 1. Biometric and Climatic Characteristics of the Four Study Sites

Site name	Howland Forest	Harvard Forest	Rannells Flint Hills Prairie	Wind River Canopy Crane Research Facility
Type of ecosystem	eastern coniferous forest boreal evergreen	temperate deciduous forest mixed deciduous	C4-dominated prairie	western coniferous forest temperate evergreen
State, country	ME, USA	MA, USA	KS, USA	WA, USA
Location (°N, °W)	45.204, 68.740	42.538, 72.171	39.12, 96.533	45.821, 121.952
Elevation (m asl)	60	340	324	355
Dominant species	Picea rubens, Tsuga canadensis	Quercus rubra, Acer rubrum	Andropogon gerardii, Sorghastrum nutans, Andropogon scoparius	Pseudotsuga menziesii
Subdominant species	Abies balsamea, Pinus strobus, Thuja occidentalis, Acer rubrum	Betula papyrifera, Betula nigra, Tsuga canadensis	Carex sp., Vernonia baldwinii, Artemesia ludoviciana, Ambrosia psilostachya and Psoralea tenuiflora var. floribunda	Tsuga heterophylla, Thuja plicata
Age (years)	140	80.5	annual	>500
Canopy height (m)	20	23	0.6	62
Mean annual temperature (°C)	6.1	6.5	13.0	8.7
Mean annual precipitation (mm)	988	1000	878	2223
Range of ABL height (m asl)[a]	920–1700	950–1900	560–1700	400–1380

[a]The range shown here were monthly estimates from ECMWF Interim Analysis data.

Glass Co., Vineland, NJ). Each week, two pairs of flasks (i.e., four flasks per week) were collected in the midafternoon on two different days (usually 3 days apart) from an intake 2 m above the top of the canopy. Sampling at midafternoon (halfway between solar noon and sunset) takes advantage of strong convective mixing that minimizes vertical CO$_2$ gradients in the ABL [*Bakwin et al.*, 1998; *Yi et al.*, 2001]. Air samples were shipped to the Stable Isotope Ratio Facility for Environmental Research at the University of Utah for laboratory analyses. A GC-IRMS system was used to analyze $\delta^{13}C$, $\delta^{18}O$ and mixing ratios of atmospheric CO$_2$ [*Schauer et al.*, 2005]. The stable isotope data will be reported in a separate paper. The precision of the CO$_2$ mixing ratios was 0.48 ppm, traceable to the WMO scale based on calibration performed against five primary standards (cylinder serial numbers: CC153217, CC153264, CC163396, CC163398 and CC163466) measured by WMO Central Calibration Laboratory for CO$_2$ in NOAA/GMD, Boulder, CO, USA.

[13] Data screening was carefully performed based on both measurements of CO$_2$ mixing ratio and carbon-13 ratio. Data were excluded if the standard deviation of a flask pair exceeds more than five times of the instrument precision (i.e., > 2.5 ppm and > 0.3‰) [*Lai et al.*, 2006a]. This selection criterion resulted in almost 13% of the samples being excluded from further analysis.

2.4. Estimates of Flux Density

[14] Estimates of monthly net CO$_2$ fluxes (i.e., equation (3)) depend on a reliable estimate of the rate of exchange between the free troposphere and the ABL (ρW_{FT}). Several authors have used different methods for estimating ρW_{FT}. *Helliker et al.* [2004] analyzed water vapor balance in the ABL to estimate ρW_{FT} and applied derived ρW_{FT} to estimate CO$_2$ exchange by assuming a similarity between CO$_2$ and water vapor transfer. *Bakwin et al.* [2004] used NCAR/NCEP Reanalysis model data [*Kalnay et al.*, 1996] to estimate ρW_{FT}. *Lai et al.* [2006a] compared monthly ρW_{FT} values predicted by the NCEP Reanalysis and European Center for Medium-Range Weather Forecasts Reanalysis (ECMWF ERA-40). Predicted $\overline{\rho W_{FT}}$ values showed very similar seasonal patterns and their monthly values generally agreed within 0.1 mol m^{-2} s^{-1}. This agreement lent support to using predicted ρW_{FT} values from the NCEP Reanalysis. *Bakwin et al.* [2004] used monthly means of the *absolute* value of daily vertical velocity to represent $\overline{\rho W_{FT}}$ in their model calculation. Their approach increased the magnitude of monthly averaged ρW_{FT} values, but no physical interpretation was given as to why absolute values of daily ρW_{FT} were used. *Lai et al.* [2006a] suggested using only *negative* (subsidence) daily ρW_{FT} values from the NCEP Reanalysis model data. Their rationale was consistent with the equilibrium BL hypothesis that the ABL dynamics reach a steady state when averaged over synoptic events [*Betts and Ridgway*, 1989; *Betts*, 2000]. This assumption is more likely to be valid when a high-pressure system prevails, in which case entrained air (negative vertical transport) allows the ABL to grow. *Helliker et al.* [2004, 2005] showed that by including only values in fair weather conditions (when subsidence dominates), the magnitude of ρW_{FT} increased and estimates of regional CO$_2$ fluxes in general had a better agreement with tower fluxes. This choice of *negative* daily ρW_{FT} values was analogous to
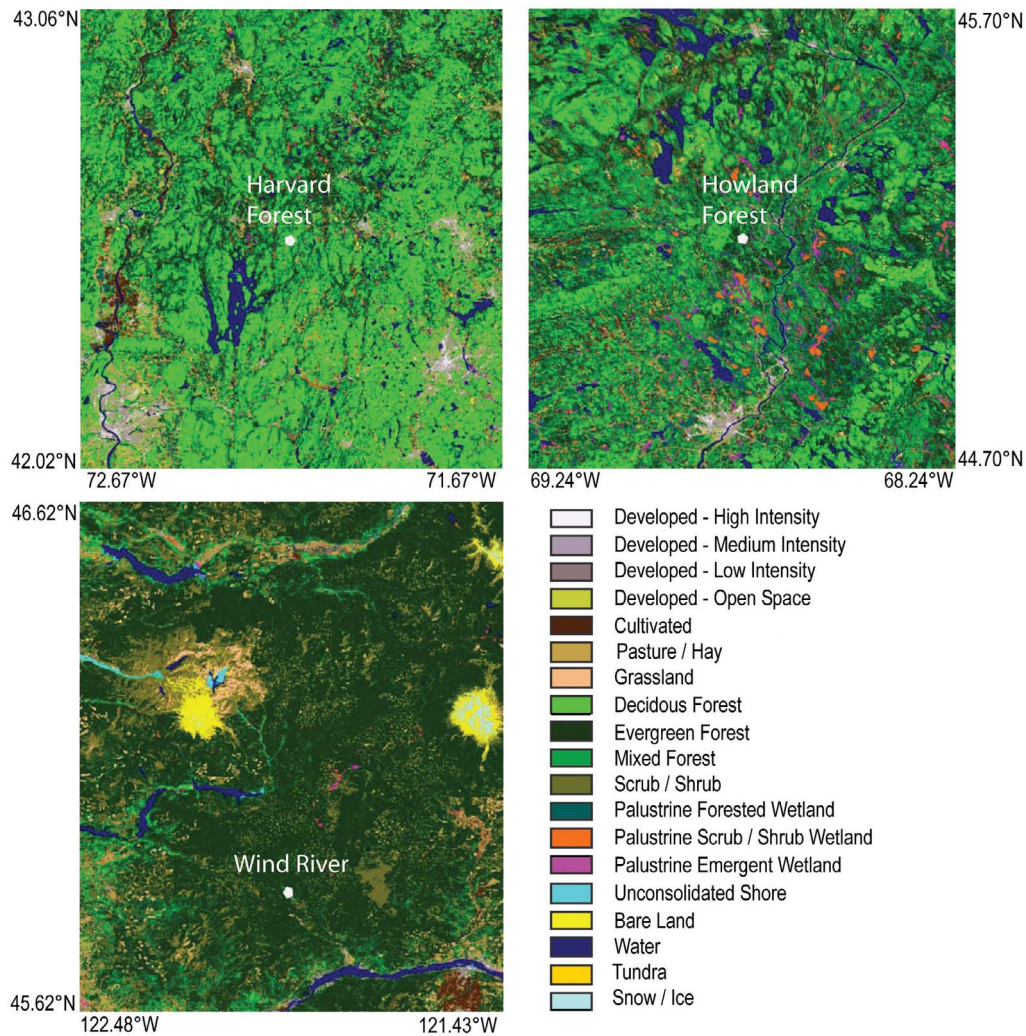
Figure 1. Maps of land use classification for the regions surrounding the three forest sites in our study. Data were provided by NOAA Coastal Services Center (http://www.csc.noaa.gov).

the argument of constraining the analysis to fair weather conditions.

[15] To account for the seasonal rectifier effect, we obtained monthly average ABL heights from the ECMWF Interim Analysis for each of the 4 study areas. We then interpolated ρW_{FT} values to the top of the ABL height following the suggestion by *Lai et al.* [2006a].

2.5. EC-MOD Upscaling

[16] *Xiao et al.* [2008, 2011] used a data-driven approach to upscale flux observations from towers to the continental scale and produced continuous NEE estimates with high spatial (1 km) and temporal (8 day) resolution for the conterminous United States over the period 2000–2006. These continuous flux fields are constrained by EC flux measurements and MODIS data streams, and are referred to as EC-MOD hereafter. In this study, we extracted windows (or regions) of different sizes (10^0 km², 10^1 km², 10^2 km², ..., 10^5 km²) surrounding each of the four towers (Table 1 and Figure 1) from the EC-MOD flux estimates [*Xiao et al.*, 2011]. The EC-MOD approach provides estimates of ecosystem carbon exchange without considering fossil fuel emissions in each

pixel. Therefore, for each flux tower, a change in the EC-MOD predicted NEE among the spatial windows (10^0–10^5 km²) most likely reflects changes in land cover, phenology, and micrometeorological conditions away from the tower.

3. Results

3.1. CO₂ Mixing Ratios in the Surface Layer and Free Troposphere

[17] Time series of CO₂ mixing ratios in the surface layer were constructed from 16 to 20 midafternoon air samples each month. This discrete sampling strategy has been shown to adequately capture major mass exchange events that are most likely to impact seasonal patterns of surface photosynthesis and respiration [*Bakwin et al.*, 2004; *Helliker et al.*, 2004; *Lai et al.*, 2006a]. Figure 2 compared seasonal fluctuations of CO₂ mixing ratios observed in each of the four study sites over the 6 years. Superimposed on the measurements were smooth curve fittings of the data using the approach developed by *Thoning et al.* [1989]. The curve fit function consists of a second-order polynomial and six
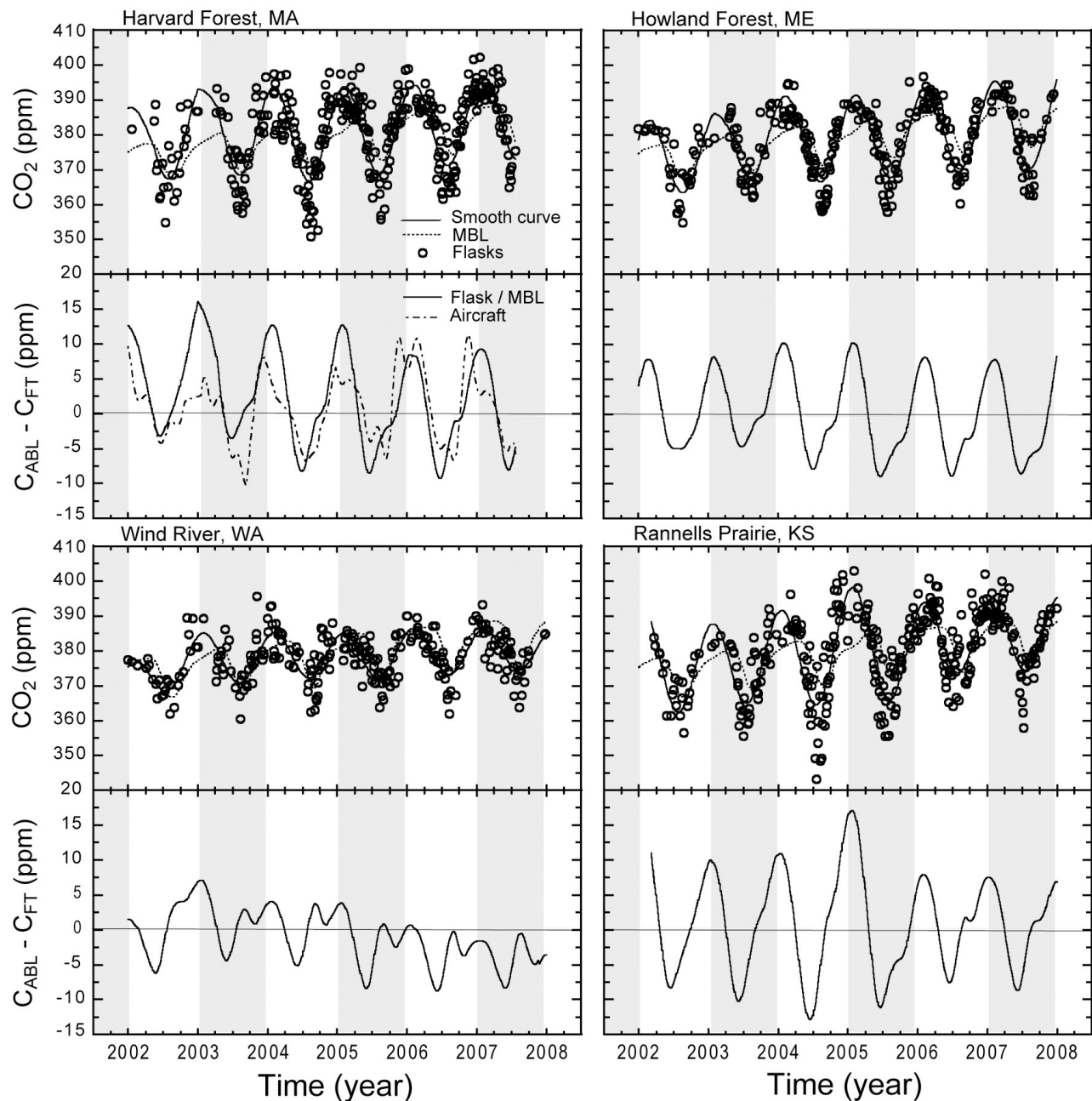
Figure 2. Midday CO$_2$ mixing ratios measured in the atmospheric boundary layer (ABL) and the differences compared to the free troposphere (FT). Open circles represent samples collected in the canopy surface layer fitted with a smooth curve (solid line). Values in the free troposphere were represented by the Globalview MBL reference data (dotted line). Also shown are aircraft measurements above the Harvard forest (dashed lines).

annual harmonics. Seasonal variations in CO$_2$ mixing ratios were much more pronounced for observations near the surface than in the troposphere, a result arising primarily from the strong influence of photosynthesis and respiration by the underlying vegetation and soil microorganisms, but also influenced by the atmospheric rectifier effect [*Denning et al.*, 2003]. Among the four sites, Harvard Forest and Wind River Forest had the greatest and smallest magnitude in the seasonal fluctuation respectively, whereas the Rannells Prairie had the largest interannual variability (represented by 1 SD of

monthly averages; the greatest was 7.0 ppm in August) during the 6 years.

[18] Figure 2 also shows the difference between smooth-curve CO$_2$ mixing ratios in the surface layer and those in the free troposphere over the 4 flux towers. The latter was approximated by marine boundary layer (MBL) reference data extracted from the Globalview-CO$_2$ database [*GLOBALVIEW-CO2*, 2009; *Masarie and Tans*, 1995]. Aircrafts have been routinely used for measuring tropospheric CO$_2$ mixing ratios over Harvard Forest (data acces-
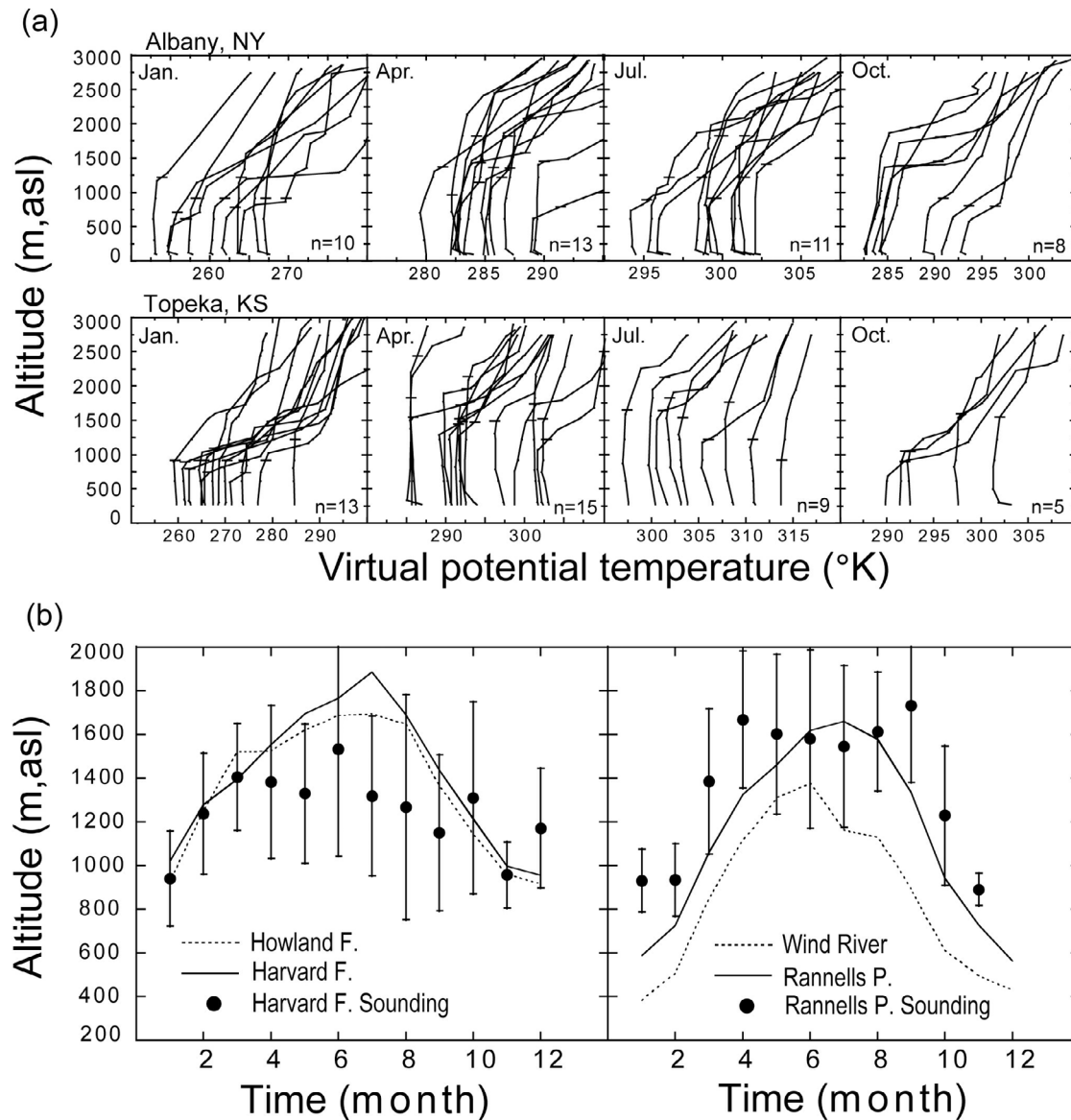
Figure 3. (a) Examples of the virtual potential temperature (°K) profiles from the sounding measurements near the Harvard Forest and Rannells Prairie sites. Sounding data at 00:00 GMT were extracted from the Albany, New York (42.70°N, 73.83°W, elevation = 96 m) and Topeka, Kansas stations (39.07°N, 95.62°W, elevation = 270 m), respectively, in the database administered by the Department of Atmospheric Science, University of Wyoming (http://weather.uwyo.edu/upperair/sounding.html). The horizontal mark in each profile indicates objectively determined maximum CBL height at that time, roughly equal halfway between the bottom and the top of the transition layer [*Fitzjarrald and Garstang*, 1981]. The n value in each figure shows the number of days when a capping inversion could be identified in each month. (b) Modeled maximum CBL height for the four study areas from the ECMWF Interim Analysis. Each line represents a composite estimate of the modeled values averaged over 6 years (2002–2007). For comparison, monthly averages of the CBL height from the sounding measurements are also shown as symbols for the Harvard Forest and Rannells Prairie sites.

sible at http://www.esrl.noaa.gov/gmd/dv/ftpdata.html). We also compared this independent measure with the MBL reference data for this site.

[19] We assume that afternoon mixing ratios measured on flux towers are representative of the ABL when integrated on a month basis. By this interpretation, a CO_2 drawdown ($C_m - C_{FT} < 0$) in the ABL can be explained as the seasonal dominance by photosynthesis whereas a CO_2 release ($C_m - C_{FT} > 0$) is associated with seasonal dominance by respiration. This assumption was supported by results from tall tower studies [*Yi et al.*, 2001, 2004]. Figure 2 shows that among the four sites, Rannells Prairie had the greatest magnitude in the seasonal fluctuation (peak-to-peak CO_2 drawdown and release, 19.5 ppm), followed by Harvard Forest

Table 2. Modeled NEE Uncertainty Shown as the Difference Between Each Scenario Relative to Those Generated by a Standard Model Run[a]

2004 Month	BL Height by Sounding		BL Height at 700mb		BL Height at 925mb	
	HV	RP	HV	RP	HV	RP
1	−0.07	0.09	0.16	−0.44*	0.27	0
2	−0.02	0.11	−0.15	−0.72*	0.35	0
3	0.00	0.26*	−0.14	−0.76*	0.24*	0.31*
4	−0.01	0.08	−0.08	−0.29*	0.19	0.3*
5	0.00	−0.03	−0.01	0.27*	0.05	−0.4*
6	0.02	0.03	0.05	0.74*	−0.27*	−1.38*
7	0.05	0.12	0.04	0.92*	−0.5*	−1.88*
8	0.06	−0.02	0.07	0.62*	−0.4*	−1.14*
9	0.03	0.01	0.03	−0.03*	−0.08*	0.04
10	0.02	0.49*	−0.13	−1.31*	0.12	0.38*
11	−0.02	0.40*	−0.33*	−2.36*	0.14	0.02
12	0.11	n/a	−0.31*	−1.71*	0.12	0

[a]Uncertainty larger than 10% of the monthly average was marked with an asterisk (HV, Harvard Forest; RP, Rannells Prairie).

(17.6 ppm), Howland Forest (13.9 ppm) and Wind River Forest (8.7 ppm). A precipitation anomaly in 2004 was mainly responsible for the large seasonal variability in the Rannells prairie during the study period [*Lai et al.*, 2006b]. If this single year was excluded, Harvard Forest consistently showed the greatest seasonal variability in the difference between CO$_2$ mixing ratios measured near the surface and those in the free troposphere.

[20] Previous studies have cautioned about inferring regional terrestrial fluxes from MBL reference data. *Gerbig*

et al. [2003] compared MBL reference data and aircraft measurements of flight tracks over the United States and southern Canada. These authors reported that aircraft CO$_2$ mixing ratios measured 3 km aboveground were consistently 0–3 ppm greater than MBL reference values, leading them to suggest that significant seasonal biases may occur if MBL reference data were used to infer regional CO$_2$ fluxes. To address this potential bias, we compared CO$_2$ differences between the ABL and free troposphere from the two estimates (Figure 2). Aircraft measurements taken at 1 km and 3 km were used to represent average CO$_2$ mixing ratios in the ABL and the lower free troposphere respectively. The two methods showed considerable discrepancies in the seasonal drawdown and release of ABL CO$_2$. In all but one year, aircraft-based estimates of summer CO$_2$ drawdown were smaller (~5 ppm) than those derived from the flask/MBL method. These discrepancies contribute proportionally to the difference in the predicted fluxes by the equilibrium BL method, as discussed later.

3.2. Boundary Layer Height and Flux Density

[21] At a given site, the height of the ABL varies diurnally as a result of surface heating and radiative cooling. On seasonal time scales, variations in the BL height have been shown to covary with surface CO$_2$ exchange, leading to biases in regional estimates of carbon flux (rectifier effect [*Denning et al.*, 1996]). On days when the convective boundary layer is well developed with an inversion cap that can relatively easily be identified, a BL height can be objectively determined from sounding profile measurements of potential temperature
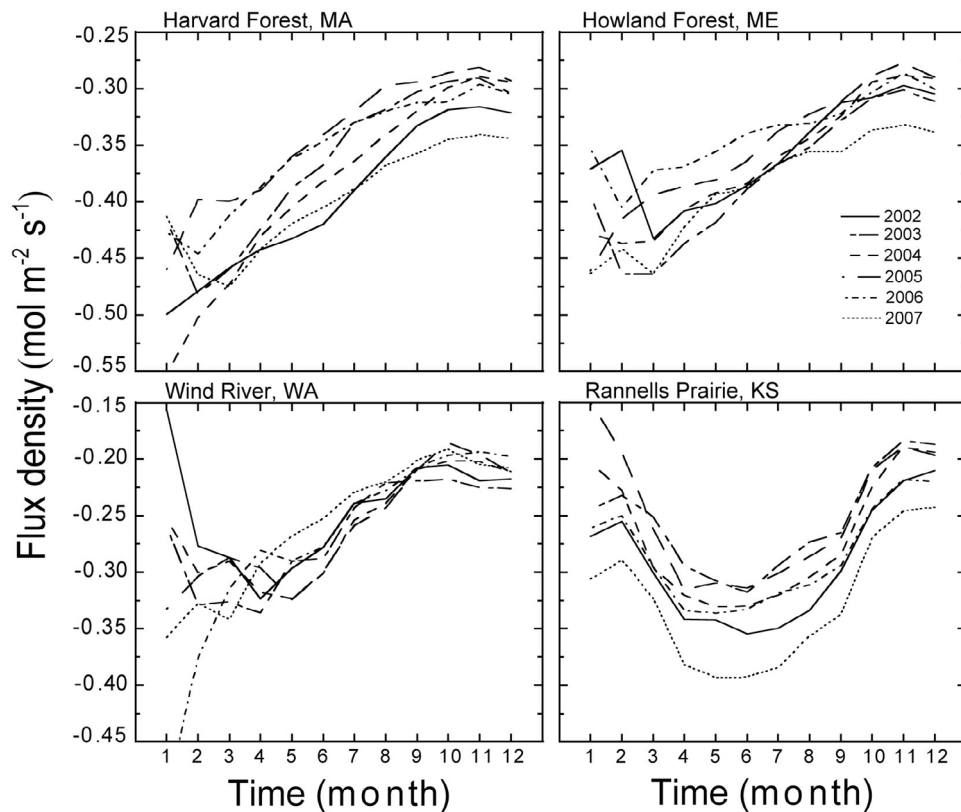

Figure 4. Seasonal variations in monthly averages of flux density from 2002 to 2007 estimated by the NCAR/NCEP and ECMWF Reanalysis data.
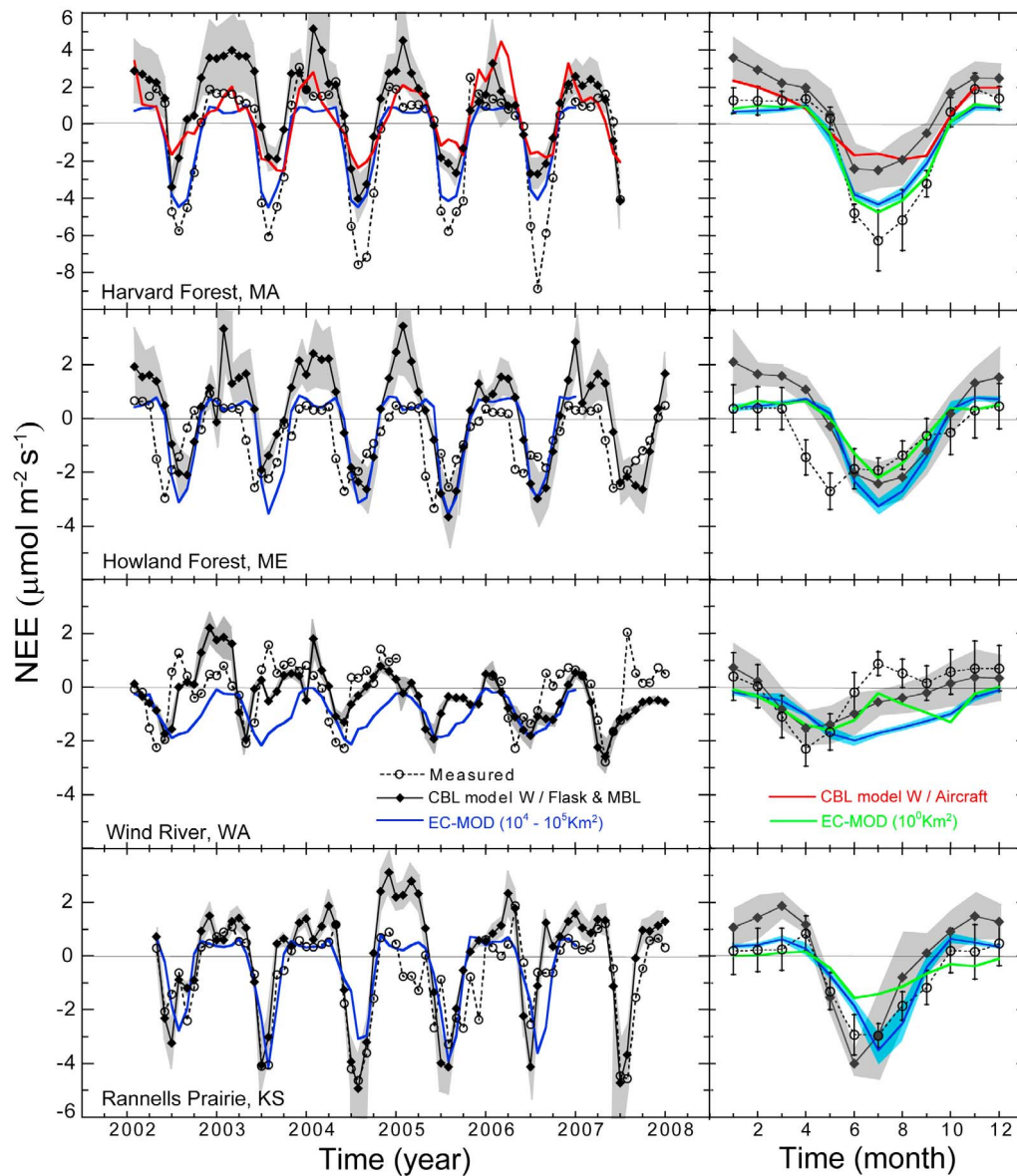
Figure 5. Comparisons of (left) interannual and (right) seasonal NEE flux estimates by the CBL model, EC-MOD approach, and tower eddy covariance. Both modeled and measured CO$_2$ fluxes were presented as monthly averages. The maximum likely errors in the CBL model flux were shown as shaded areas in the left column. The EC-MOD model flux shown in the left column includes pixels representing an area on the order of 10^4–10^5 km^2 centering on the tower. The shaded areas in the right column represent 1 SD of the ensemble average over the 6 years (without propagation) for the CBL model in gray, EC-MOD of 10^0 km^2 in green and EC-MOD of 10^4–10^5 km^2 in blue.

and water vapor [*Fitzjarrald and Garstang*, 1981; *Melgarejo and Deardorff*, 1974]. We examined virtual potential temperature (θ) profiles near Harvard Forest and Rannells Prairie day-by-day, selecting the days when a capping inversion was visually identifiable. We then separated these profiles by months. An example of the θ profiles is shown in Figure 3a to demonstrate the concept. The number of days when a capping inversion was visually identifiable in a month varied from 5 to 17 days near Rannells Prairie, and from 5 to 13 days near the Harvard Forest. We calculated monthly average BL heights from these daily sounding profiles for each of the months in

2004, and compared them to those derived from the ECMWF model. Figure 3b shows this comparison. ECMWF-modeled BL depths showed a better agreement for the prairie site than the Harvard Forest by capturing seasonal variations similar to those in the sounding data. The ECMWF model over-predicted the BL depth during summer at the Harvard Forest. The sounding-based BL depth showed a seasonal pattern that was in close agreement with that reported by *Freedman et al.* [2001], despite having higher values (1200 m versus 1000 m) during summer months. Taken together, the standard deviation of the sounding-based BL depths often exceeded 300 m

around the monthly average. This uncertainty introduced relatively small errors in the BL model NEE (Table 2).

[22] *Bakwin et al.* [2004] selected ρW_{FT} values at a fixed height from NCEP Reanalysis (i.e., without considering the rectifier effect) to estimate monthly NEE for an entire year in four flux tower sites that include Harvard Forest. The NCEP Reanalysis only predicted ρW_{FT} at discrete altitudes (e.g., 700mb, 850mb and 925mb in the current study), unable to resolve seasonal variations in the rate of vertical exchange between the free troposphere and the ABL. In the present study we considered the seasonal rectifier effect by scaling ρW_{FT} to modeled maximum BL heights obtained from the ECMWF Interim Analysis. Following *Lai et al.* [2006a], we used a composite, monthly estimate of the modeled BL heights to scale ρW_{FT} and account for the seasonal variability in the depth of the CBL (Figure 3). This approach was evaluated and shown to produce reasonable estimates of BL heights that varied over seasons, and as a result, improved the predicted seasonality of surface CO$_2$ fluxes in the Rannells Prairie in a previous study [*Lai et al.*, 2006a].

[23] Figure 4 shows modeled seasonal variability in the flux density. In general, the lowest ρW_{FT} (strongest subsidence) occurred in spring. Howland Forest and Harvard Forest had lower ρW_{FT} values than Rannells Prairie and Wind River. Within a site, interannual variability was generally smaller than seasonal variability. The effect of this variability on modeled fluxes was examined by a sensitivity analysis discussed later.

3.3. Comparison of Net CO$_2$ Fluxes

[24] Figure 5 showed the comparison between modeled and measured monthly NEE. Here, negative fluxes indicate carbon uptake by an ecosystem. This cross-site comparison showed three general patterns between BL modeled and tower NEE fluxes. First, BL modeled wintertime NEE were greater than EC-MOD and tower NEE at all sites in almost all the study years. Second, modeled and measured NEE showed varying agreement among sites, with closer agreement found in Rannells Prairie and Wind River Forest. Third, modeled and measured NEE showed considerable disagreement in the two northeastern U.S. forests resulting from different reasons. Modeled summertime uptake, regardless of the method used to calculate CO$_2$ differences between ABL and the free troposphere, was consistently smaller than tower NEE in Harvard Forest. At the Howland Forest, the magnitude of modeled summertime uptake was similar to that observed by the tower. However, modeled CO$_2$ fluxes at this site showed a lag in the peak of growing season uptake by 2 months behind that of tower measurements (from May to July). Such a phase shift in the modeled seasonal fluxes was not apparent in the comparison of the other three sites.

[25] The EC-MOD fluxes averaged over an area of the order of 10^4–10^5 km^2 generally agreed with the results from the BL model. In particular, both models predicted the same disagreement compared to the tower NEE at the two northeastern U.S. forests. At all sites, modeled summertime NEE decreased in magnitude as the size of the window surrounding the tower increased from 10^0 km^2 to 10^5 km^2 in the EC-MOD. The discrepancy between EC-MOD and tower NEE became greater as the window size increased. At the Wind River site, increasing the size of the window drastically

augmented the discrepancy in the predicted seasonal pattern. At the other three sites, by contrast, changes in the size of the window did not substantially influence the differences between EC-MOD and tower NEE.

4. Discussion

[26] In this study we modeled regional CO$_2$ fluxes by inferring midday mixing ratios measured in the canopy surface layer at 4 flux stations over 6 years. We applied the equilibrium boundary layer concept to focus on monthly CO$_2$ balance, using readily available, community model outputs to provide a systematic, cross-site evaluation of model performance. This simple approach does not allow for investigating biological controls of surface fluxes over periods that are shorter than synoptic scales. However, a multiyear comparison provides useful information for understanding the influence of climate forcing on interannual variability of land surface fluxes. A cross-site synthesis enables us to further distinguish uncertainties associated with inherent model assumptions from representation errors associated with spatial heterogeneity near a flux tower. To put our interpretation of the model NEE in context, we performed a suite of uncertainty analyses.

4.1. Sensitivity and Error Analyses
4.1.1. Uncertainty Associated With Smooth Curve Fitting

[27] To evaluate the effect of smooth curve fitting to the CO$_2$ time series on the modeled NEE, we reran the model using flask CO$_2$ mixing ratios (without smooth curve fitting) and compared the modeled NEE with a standard run (smooth curve fitted CO$_2$ time series). Using smooth curve CO$_2$ time series generally resulted in NEE differences < 0.5 μmol m^{-2} s^{-1} in the three forest sites, and < 1.0 μmol m^{-2} s^{-1} in the Rannells Prairie. These errors were comparable to other types of errors (Figure 6, discussed later). Modeled NEE differences randomly clustered around zero (the largest mean was -0.04 ± 0.48 μmol m^{-2} s^{-1} among the four study sites), suggesting that there was no systematic bias in the modeled NEE with respect to smooth curve fitting. Smooth curve fitting also did not influence the seasonal pattern in the model NEE, consistent with the results shown by *Lai et al.* [2006a].

4.1.2. Uncertainty Associated With Error Interactions in the Equilibrium BL Model

[28] The simplified equilibrium BL model predicts fluxes as the product of two parameters: flux density and the CO$_2$ mixing ratio gradient between the mixed layer and the free troposphere. This two-parameter model makes error interaction analysis relatively straightforward. We allow the errors in the two parameters to interact, and consider 4 combinations of the interaction between errors around the two parameters, namely, positive × positive, positive × negative, negative × positive and negative × negative. For each interaction, we reran the model and calculated monthly fluxes at each site for all 6 years. For this analysis, errors associated with mixing ratios were evaluated by altering measured values by the instrument precision (± 0.5 ppm). Errors associated with flux density were evaluated by ± 1 SD of the ensemble monthly average for the 6 study years. The largest errors found among the 4 interaction runs were shown as shaded areas in Figure 5.
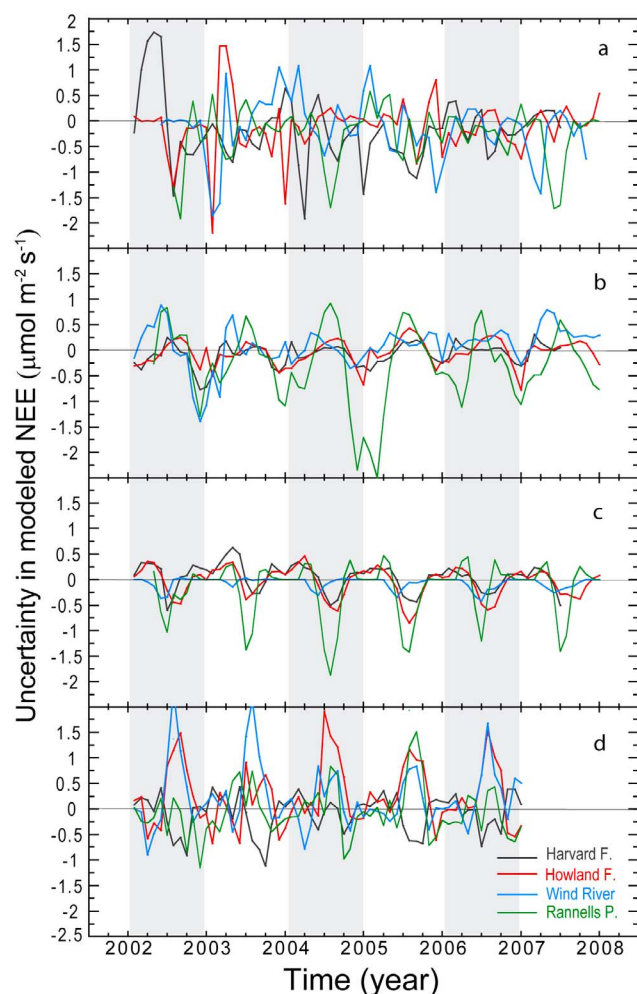
Figure 6. Potential errors in the model CO_2 fluxes. Errors in the BL model were calculated by three scenarios: (a) using air samples collected only under fair weather conditions, (b) assuming constant flux density at 700 mb level, and (c) assuming constant flux density at 925 mb level. Errors were represented by the NEE difference from the standard model run (all weather, seasonally variable flux density; see Figure 5). (d) NEE difference in the EC-MOD model between two spatial scales (10^0 km² minus 10^4 km²).

4.1.3. Uncertainty Associated With the Fair Weather Assumption

[29] We performed a second set of uncertainty analyses to account for the potential errors in the estimate of BL height and the fair weather assumption imposed by the equilibrium BL model. By employing the equilibrium BL concept our approach assumed that an idealized mixing layer model was able to produce NEE fluxes representative of a period averaged over synoptic weather events, an assumption that has not been verified. A major issue with the assumption is determining *when* an idealized equilibrium BL exists. *de Arellano et al.* [2004] used aircraft measurements and a mixed layer model to investigate the ABL CO_2 budget on the diurnal scale. Under an idealized condition, these authors found that surface CO_2 fluxes and air entrainment at the top of the ABL were nearly in balance. The equilibrium BL model

hypothesizes that the ABL reaches a steady state between surface fluxes, cloud effects on radiation, and subsidence of the overlying free troposphere when averaged over longer timescales [*Betts and Ridgway*, 1989; *Betts*, 2000]. This assumption is more likely met only on days of fair weather. An idealized mixed layer model breaks down outside these limited boundary layer conditions when the horizontal convection cannot be assumed negligible. *Teixeira et al.* [2008] reviewed some general challenges in the parameterization of the atmospheric boundary layer. To evaluate the model sensitivity associated with this assumption, we arbitrarily defined fair weather conditions as days of measurable precipitation of less than 1 mm, and then removed air samples collected on days when measured precipitation was > 1 mm. This resulted in 30% of the samples being excluded from the complete CO_2 data. We reran the model and compared the results to those generated by a standard model run (all weather, seasonally variable flux density). Figure 6a shows the NEE difference from this comparison. Subsampling CO_2 data notably altered the modeled NEE, particularly in months when the number of data points was significantly reduced in the model. The errors randomly clustered around zero (the largest mean was -0.28 ± 0.54 μmol m^{-2} s^{-1} among the four study sites), suggesting that there was no systematic bias in our modeled CO_2 fluxes with respect to the fair weather assumption. Our analysis suffered from the limited number of flask air samples; despite high precision and additional information (stable isotope analysis). In that regard, there is a real advantage of conducting in situ, high precision CO_2 mixing ratio measurements at flux towers [*Wang et al.*, 2007; *Yi et al.*, 2004].

[30] Because the BL model only considered fair weather conditions, modeled CO_2 fluxes should strictly be compared to tower NEE measured in the same condition [*Lai et al.*, 2006a]. However, as *Lai et al.* [2006a] pointed out, subsampling the fair weather tower NEE only resulted in modest differences when compared to those including all weather conditions. In the present study, we recalculated monthly average tower NEE after excluding days when daily cumulative precipitation was > 1 mm for the three forest sites (*Lai et al.* [2006a] performed a similar analysis for the Rannells Prairie). We found that subsampling the fair weather only resulted in modest differences (<5%) when compared to all weather NEE. This small difference likely resulted partially from the fact that many of the gap-filling functions were developed on the basis of fair weather conditions, and the gap-filled data only represented a small portion of the complete data. *Lai et al.* [2005] provide a review of the gap-filling methods used in our four study sites.

4.1.4. Uncertainty Associated With the BL Height

[31] A second major issue with respect to the equilibrium BL assumption is how to obtain a representative estimate of the BL height, as a well-developed capping inversion in the ABL does not exist on a daily basis. *Denning et al.* [2008] compared simulated PBL depth with radar profile measurements at the WLEF tower in northern Wisconsin, United States, observed during 1999. Their results showed a general trend that underestimates the PBL depth during growing season. The authors concluded, "it is unlikely many models can reproduce the rapid changes and strong diurnal and synoptic variations in the PBL depth." Determining an

objective BL height for an averaging time interval over which the ABL approaches an equilibrium state presents a major source of uncertainty in our model.

[32] In the present study, we used modeled maximum BL height from the ECMWF Interim Analysis to represent the average ABL depth on monthly time scales. The modeled maximum BL height likely exceeded average BL height at a given site. For example, *Freedman et al.* [2001] reported a seasonal trend of the mixed layer height over the Harvard Forest. They observed highest mixed layers (~1350 m) occurring in the late spring, near the time of maximum springtime sensible heat flux. The ECMWF composite BL height showed a seasonal variation ranging from 950 m during the winter months to 1900 m during the summer. *Holzworth* [1972] reported a range of the BL height in Albany, NY, changing from 900 m during the winter to 1800 m during the summer. The ECMWF composite estimates agreed with those reported by *Holzworth* [1972], but were contrary to the seasonal pattern shown by *Freedman et al.* [2001]. *Freedman et al.* [2001] discussed the disparity in the seasonal pattern of the BL height observed for this site. According to *Freedman et al.* [2001], *Holzworth*'s [1972] estimates of the BL height assumed a completely adiabatic mixing, giving a maximum estimate similar to those in the ECMWF Interim Analysis. This may explain why ECMWF model BL heights were higher in the summer when compared to the sounding data at this site. By contrast, the composite BL height from the ECMWF Interim Analysis agreed very well with the sounding observation in the Rannells Prairie. Monthly variations around the average BL height often exceeded 300 m in the sounding data. This uncertainty leads to the need of a careful evaluation for its effect on the modeled NEE.

[33] We scaled ρW_{FT} to the monthly BL height estimated from the sounding data. We then reran the model for all the months in 2004. The potential errors of relying on community model outputs (i.e., scaling ρW_{FT} to the modeled BL heights) were investigated by using the BL depths from the sounding data for all months in 2004 (the year with most pronounced seasonal variations in the tower NEE during our study period, see Figures 5). Table 2 showed the NEE difference calculated as the modeled NEE subtracted by those generated from a standard model run. Replacing ECMWF BL heights by the sounding data generally resulted in NEE differences of less than ±0.1 μmol m^{-2} s^{-1}, a less pronounced error when compared to other sources of uncertainty (Table 2 and Figure 6). Combining sounding measurements wherever available with large-scale, community model outputs provide a crosscheck of the BL height estimates in atmospheric inversion analyses.

4.2. Sensitivity of Modeled NEE to the Seasonal Rectifier Effect

[34] ECMWF model data and sounding measurements both showed strong seasonal patterns of the ABL depth with higher values near the summer and lower values during the winter months. This seasonal covariance between NEE and the depth of ABL (the rectifier effect) has been shown as a major source of uncertainty in the atmospheric inversion analysis [*Denning et al.*, 1995, 1996; *Law and Rayner*, 1999]. To this end, we conducted two model scenarios to demonstrate the effect of neglecting seasonal rectifier forcing on the

modeled NEE. We evaluated ρW_{FT} outputs at 700mb and 925mb levels (roughly corresponding to altitudes 2560 m and 720 m asl respectively) from the NCEP Reanalysis to calculate NEE for an entire year without scaling to seasonal dynamics of BL depths. That is, we calculated NEE for the entire year using fixed ρW_{FT} values at either maximum (summer) or minimum (winter) BL heights, and compared the results to those generated by a standard model run. Figures 6b and 6c show the results of this comparison, respectively, for the entire study period. Neglecting seasonal variations in the BL height generally resulted in a NEE difference in the range ±0.5 μmol m^{-2} s^{-1}, except for the Rannells Prairie, where the largest difference often exceeded 1.0 μmol m^{-2} s^{-1} (Table 2). These results suggest it is important to account for the rectifier effect when applying the BL model in the North American Great Plains. By contrast, the seasonal rectifier effect is less pronounced (seasonal variations in the BL height and NEE are out of phase) in the two northeastern forest regions. *Freedman et al.* [2001] showed that in the U.S. eastern deciduous forests, highest mixed layers occur in the late spring, just before leaf emergence, months before maximum carbon uptake and minimum BL CO₂. This highest BL depth corresponds with the maximum springtime sensible heat flux and the highest Bowen ratio. We postulate that the ECMWF's overprediction of summertime BL heights likely results from a misrepresentation of the deciduous phenology. Furthermore, neglecting the rectifier effect resulted in systematic seasonal biases in the model NEE. At all sites, without considering seasonal variations in the BL height, the BL model tended to overestimate summer net CO₂ uptake and underestimate wintertime fluxes. The stronger the rectifier forcing, the more pronounced is the NEE bias in the model, consistent with the pattern shown in the GCM transport inversion study [*Gurney et al.*, 2003].

4.3. Comparison of Modeled NEE With the EC-MOD Approach

[35] We compared the BL model NEE with the EC-MOD fluxes at two spatial scales. The results were shown as the difference (10^0 km^2 minus 10^4 km^2) in Figure 6d. The two scales were selected to resemble those of the tower and BL modeled NEE, respectively. NEE differences between the EC-MOD scenarios mainly reflect changes in the forest cover, land use type and environmental forcing that drive the underlying biotic activity [*Xiao et al.*, 2011]. The discrepancy between tower NEE and EC-MOD fluxes generally became greater as the window included a larger area (Figure 5). At flux stations located in areas of high heterogeneity (diversity of plant species, stand age, microclimate, topography, soil types, land use), such spatial variation might have enhanced the discrepancy between EC-MOD NEE. This can explain the larger variation found in Rannells Prairie, Wind River, and the Howland Forest (Figure 6d). For the Harvard Forest, summertime CO₂ uptake decreases as the size of the window increases, consistent with the results predicted by the BL model. Fossil fuel emission likely contributes to the discrepancy at this site, as has been shown by previous studies [*Bakwin et al.*, 2004; *Lai et al.*, 2004]. According to the 1 km-resolution MODIS land cover map, urban areas account for 5.6% of the region (10^4 km^2) but the percentage drops to nearly 0 when the footprint is 10^3 km^2 or smaller centered on the Harvard Forest flux tower. Because EC-MOD does not

consider fossil fuel emission, Figure 6d suggests biogenic factors also contribute to the discrepancy between the tower and modeled CO_2 fluxes.

4.4. Attributes of the Differences Between Modeled and Tower NEE

[36] The two independent modeling approaches show remarkable agreement for the regional-scale estimate of net CO_2 fluxes during the study period (Figure 5). This multitechnique, cross-site comparison provides insights into causes responsible for the observed discrepancy, and sheds light on the deficiency of each model. We observed two types of systematic differences between modeled net CO_2 fluxes and tower measured NEE. The first type of systematic differences was found in the wintertime fluxes, in which BL model fluxes were consistently larger than tower NEE at all but Wind River site. The EC-MOD approach consistently predicted wintertime fluxes closer to the tower measurements than the BL model, irrespective of EC-MOD spatial scale. This discrepancy of wintertime fluxes at least partially resulted from the greater anthropogenic (fossil fuel CO_2, domestic heating from biomass burning, etc) influence on regional mixing ratios than tower fluxes, which has been demonstrated previously in the Harvard Forest [*Bakwin et al.*, 2004] and Rannells Prairie [*Lai et al.*, 2006a]. Using carbon monoxide (CO) mixing ratio measurements and an emission ratio $CO/CO_2 = 20:1$ (ppb/ppm), these authors estimated monthly combustion of $0.3–1.0$ μmol m^{-2} s^{-1} and $0–0.5$ μmol m^{-2} s^{-1} at the two sites, respectively. Considering the contribution of fossil fuel CO_2 fluxes helps reconcile the discrepancy reported here. Wind River Forest appears to be less susceptible to the direct influence of anthropogenic CO_2. We did not conduct the fossil CO_2 analysis for the Howland Forest. Therefore we can only speculate that fossil fuel CO_2 fluxes may also be an important contributor to the modeled winter fluxes in that region.

[37] The second type of systematic differences results from the scale mismatch between tower and model footprints. Inversion models relying on mixing ratio observations have often reported smaller fluxes when compared to tower-based NEE measurements [*Chen et al.*, 2008; *Desjardins et al.*, 1992]. *Gioli et al.* [2004] compared tower and aircraft-based eddy covariance fluxes in 5 European regions and found good agreement between the two types of measurements only when flights were at heights comparable to the tower height over relatively homogeneous stands. Their findings clearly demonstrate the inherent difference, as a result of the footprint effect, between tower and inversion estimates of CO_2 fluxes. The EC-MOD approach, when evaluated in a wide range of spatial scales, provides an excellent tool to crosscheck inversion results. In turn, combining tower and BL flux estimates offers constraints at two distinct spatial scales for remote sensing-based upscaling approaches.

[38] Merits and limitations of each approach have been discussed in depth elsewhere [*Baldocchi et al.*, 2001; *Dolman et al.*, 2009; *Gamon et al.*, 2006b; *Mahrt*, 1998; *Xiao et al.*, 2008, 2011]. Factors that contribute to the uncertainty in tower eddy CO_2 fluxes include but are not limited to: instrument deficiency (e.g., loss of spectrum energy under low turbulence), oversimplification in theory (e.g., zero divergence in complex terrain) and representative errors (e.g.,

tower locations not representative of dominant vegetation types). Uncertainties associated with the inverse modeling approach employed here include: errors in the CO_2 mixing ratio measurements (both near the surface and in the free troposphere), unreliable estimates of boundary layer heights and vertical transport across the top of the atmospheric boundary layer, and the assumption of an equilibrium boundary layer over time periods longer than synoptic scales. There are several sources of uncertainty associated with EC-MOD flux estimates, including uncertainties in the eddy flux measurements, land cover, model structure, representativeness of the AmeriFlux site locations [*Xiao et al.*, 2008, 2010], and finally, the exclusion of fossil CO_2 fluxes by the EC-MOD.

[39] Sensitivity analyses suggested that the discrepancy between modeled and tower NEE cannot be explained by considering uncertainties in the modeling approach alone. The phase shift in the modeled NEE at the Howland Forest likely reflects contributions from deciduous forests in the region and to the south. This seasonal signal from the U.S. northeastern deciduous forests was strongly evident in the NEE measurements from the Harvard Forest. The location of flux towers is often selected to minimize anthropogenic influences on NEE measurements and to be consistent with micrometeorological requirements. In this way, tower EC measurements can be used to investigate baseline, biophysiological relationships that shed light on ecosystem response to changes in environmental conditions; however, they may not be representative of the regional distribution of vegetation.

4.5. Toward Equilibrium H₂O and CO₂ Exchange in the ABL at Monthly Time Scales

[40] The Equilibrium boundary layer concept [*Betts*, 2000; *Priestley and Taylor*, 1972; *Raupach*, 1991] was first developed to predict surface evaporation. In the absence of horizontal convection, CBL moisture roughly reaches a balance between surface fluxes and entrainment. The basic assumption allowing the CBL to converge to equilibrium evaporation is rarely achieved on a diurnal time scale [*Raupach*, 2000], requiring averaging integrals over longer time (several days to weeks). *van Heerwaarden et al.* [2009] used model data to examine equilibrium evaporation on diurnal time scales. These authors showed that evaporation could approximate equilibrium but only momentarily. The exact averaging time interval reaching an equilibrium ABL is uncertain, and is further confounded by the synoptic weather patterns at selected study sites. The lack of a well-defined averaging interval complicates the interpretation of the modeled NEE.

[41] In this study we performed model calculations of monthly average NEE on the basis of daily CO_2 mixing ratios; missing data were gap-filled by linear interpolation between observed values. Modeled NEE were compared with tower NEE assuming ABL CO_2 exchange approaches an equilibrium state on the monthly time scale. By doing so we directly smooth out daily and synoptic variability in the weather and biotic processes. Here we explore ideas of why monthly average NEE may be appropriate.

[42] Helliker-Betts-Berry applied the equilibrium BL concept to estimate CO_2 fluxes by coupling them with H_2O exchange in the CBL over the WLEF flux tower [*Betts et al.*,

Table 3. Relationship of Interannual Variability Between Precipitation and NEE for the Four Study Sites[a]

	Harvard Forest	Howland Forest	Wind River	Rannells Prairie
Tower NEE	Slope = −1.61, $R^2 = 0.71$, $F = 0.04$	Slope = −0.16, $R^2 = 0.22$, $F = 0.35$	Slope = 0.21, $R^2 = 0.68$, $F = 0.09$	Slope = −0.94, $R^2 = 0.50$, $F = 0.11$
Modeled NEE	Slope = −0.82, $R^2 = 0.23$, $F = 0.34$	Slope = −0.02, $R^2 = 0.00$, $F = 0.97$	Slope = 0.28, $R^2 = 0.55$, $F = 0.09$	Slope = −0.82, $R^2 = 0.66$, $F = 0.05$

[a]Slopes indicate rates of change from a linear regression model NEE = slope × Precipitation + intercept.

2004; *Helliker et al.*, 2004, 2005]. Other studies [e.g., *Bakwin et al.*, 2004; *Desai et al.*, 2010; *Lai et al.*, 2006a] applied the equilibrium BL model to estimate NEE at monthly intervals but they did not adequately provide explanations to justify the use of monthly averages. One of the reasons that may explain the agreement between modeled and measured NEE is the common radiative forcing that drives the variations in surface CO$_2$ exchange and the ABL dynamics. This is analogous to the gap-filling strategy to replace missing data points in the eddy covariance measurements as a result of inclement weather. Gap-filling is desired and an important part of the standardization to enable annual carbon budget estimates and facilitate cross-site comparisons [*Baldocchi*, 2008; *Papale et al.*, 2006; *Reichstein et al.*, 2005], and has been shown to have a modest impact on annual sums of NEE [*Moffat et al.*, 2007]. The majority of gap-filling methods use 'ecophysiologically sound' nonlinear regressions parameterized on the basis of fair weather conditions (i.e., some variations of light response function for gross primary production (GPP) and temperature function for ecosystem respiration (Re), see the

review by *Moffat et al.* [2007]). Monthly averages of the gap-filled data therefore represent a mean ecosystem response to the energy (radiation and temperature) forcing.

[43] Radiative forcing also drives the BL dynamics, most pronounced diurnally (surface heating and buoyancy) and seasonally (rectifier). *Denning et al.* [2008] analyzed simulated and observed PBL depth at the WLEF tower. These authors showed that the monthly mean PBL depth, ensemble-averaged from daily estimates of mixed-layer depth by time of day in 1998, reproduced the diurnal PBL pattern typically observed only during fair weather conditions. This diurnal pattern of radiation (or photosynthetic photon flux density) was shown as a strong forcing that explains a great deal of the temporal variability in terrestrial CO$_2$ fluxes [*Baldocchi et al.*, 2001; *Katul et al.*, 2001; *Mahecha et al.*, 2010]. *Katul et al.* [2001] used power spectrum analysis to investigate the relationship between surface H$_2$O exchange and net radiation (R$_n$) in a loblolly pine (*Pinus taeda L.*) plantation at Duke Forest, North Carolina, United States. They showed that the relationship between R$_n$ and latent heat fluxes (LE) was poor
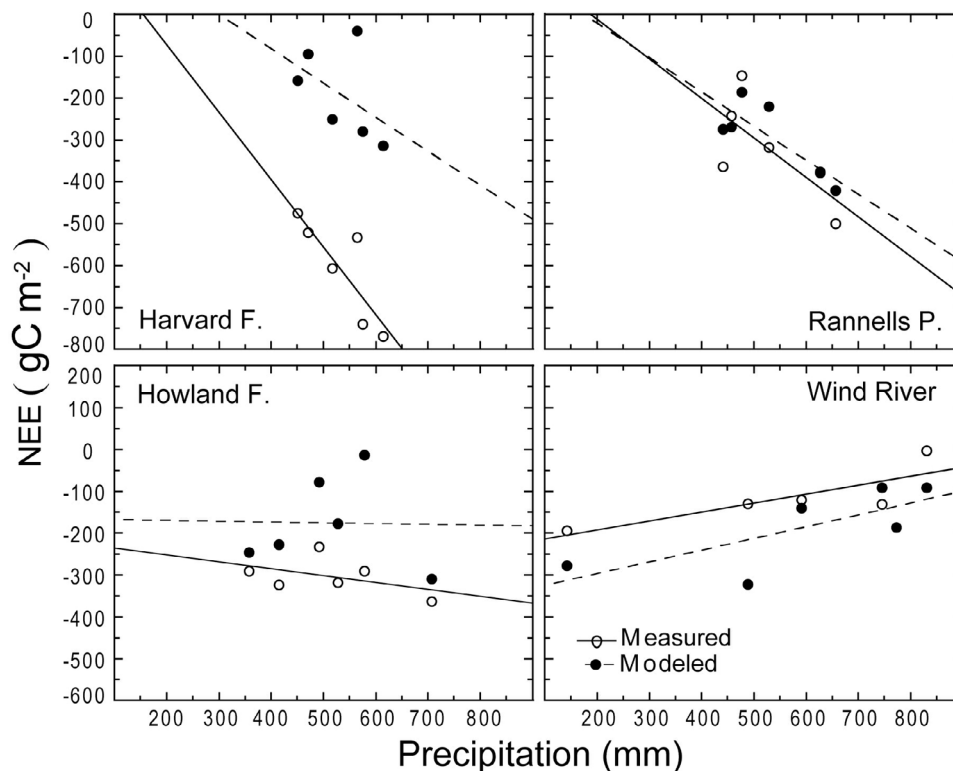

Figure 7. Relationship of interannual variability between precipitation and NEE. The precipitation and NEE values are sums over the growing season at each site (Harvard Forest and Rannells Prairie: May–September; Howland Forest and Wind River: March–September).

on half-hourly time scales, but a strong relationship exists between monthly LE and monthly R$_n$. During months of high R$_n$ (summer), the relationship between LE and R$_n$ was well described by equilibrium evaporation. *Katul et al.* [2001] also found a similar relationship for NEE. Their observations provide supporting evidence that monthly averages may be appropriate to aggregate NEE in the context of an ABL inversion analysis. We postulate that the radiation forcing acts commonly on the evolution of the ABL and NEE, enabling a direct comparison with the equilibrium BL estimates when NEE fluxes are aggregated monthly, despite the limitation that an idealized model is theoretically valid only in fair weather conditions.

4.6. Relationships Between NEE and Precipitation

[44] From 2002 to 2007, we found that growing season precipitation was an important factor explaining the interannual variability of NEE in all sites but Howland Forest (Table 3). Figure 7 and Table 2 show the comparison between these relationships. It has been well documented that the productivity of tallgrass prairies is highly sensitive to water availability [*Kim and Verma*, 1991; *Knapp*, 1984]. *Urbanski et al.* [2007] investigated the influence of soil moisture on interannual variability of NEE at the Harvard Forest and found weak correlations in measurements collected from 1992 to 2004, which contradicts the findings in the present study. Wind River Forest showed a negative relationship between the interannual variability of NEE and precipitation when compared to the other three sites. That is, higher moisture availability resulted in more carbon loss from the ecosystem. This excess loss of carbon during the growing season likely resulted from enhanced decomposition of surface litter and dead woody tissues, as summer moisture is more important to near surface soil microbes than trees in this ecosystem. For all sites, modeled NEE generally showed a weaker sensitivity to water availability. These findings demonstrate the need to carefully consider the effect of drought in the coupled carbon-climate models, as the carbon-water relationship appears to vary among sites and between scales. We did not find linear relationships between EC-MOD CO$_2$ fluxes and precipitation. Upscaled NEE by the EC-MOD had significantly smaller interannual variability compared to the other two NEE estimates (Figure 5), and did not appear to covary with the interannual variability in the growing season precipitation.

5. Conclusions

[45] A reliable regional estimate of carbon exchange is highly relevant to management and policy decisions. Efforts to improve our ability to quantify and reduce uncertainties of regional CO$_2$ budgets should be encouraged. In this paper we show that the boundary layer inversion approach can provide an intermediate-level analysis to complement aircraft or satellite based integration efforts for estimating the continental carbon budget. We suggest that the radiation forcing acts commonly on the evolution of the ABL and NEE, enabling a direct comparison with the equilibrium BL estimates when NEE fluxes are aggregated monthly. We demonstrate the site-specific importance of the seasonal rectifier effect on the regional carbon balance estimate using atmospheric inversion

technique. Neglecting the rectifier effect results in systematic seasonal biases in modeled NEE. At all sites, without considering seasonal variations in the BL height, the BL model tends to overestimate summer net CO$_2$ uptake and underestimate wintertime fluxes. The stronger the rectifier forcing, the more pronounced is the NEE bias in the model. Our results suggest it is important to account for the rectifier effect when applying the boundary layer model in the Great Plains. We show that an idealized BL model of simple parameterizations, when applied in a system manner across multiple sites, can provide valuable insights to add to the interpretation of tower flux observations. We suggest that future studies need to consider a true model fusion approach by combining multiple upscaling methods, where new insights will likely be drawn to develop routine, diagnostic tools that contribute to our understanding of the seasonal and interannual variability of surface CO$_2$ fluxes.

References

Bakwin, P. S., et al. (1998), Measurements of carbon dioxide on very tall towers: Results of the NOAA/CMDL program, *Tellus, Ser. B*, *50*(5), 401–415, doi:10.1034/j.1600-0889.1998.t01-4-00001.x.

Bakwin, P. S., et al. (2004), Regional carbon dioxide fluxes from mixing ratio data, *Tellus, Ser. B*, *56*(4), 301–311, doi:10.1111/j.1600-0889.2004.00111.x.

Baldocchi, D. (2008), Breathing of the terrestrial biosphere: Lessons learned from a global network of carbon dioxide flux measurement systems, *Aust. J. Bot.*, *56*(1), 1–26.

Baldocchi, D., et al. (2001), FLUXNET: A new tool to study the temporal and spatial variability of ecosystem-scale carbon dioxide, water vapor, and energy flux densities, *Bull. Am. Meteorol. Soc.*, *82*(11), 2415–2434, doi:10.1175/1520-0477(2001)082<2415:FANTTS>2.3.CO;2.

Battle, M., et al. (2000), Global carbon sinks and their variability inferred from atmospheric O$_2$ and δ^{13}C, *Science*, *287*(5462), 2467–2470, doi:10.1126/science.287.5462.2467.

Betts, A. K. (2000), Idealized model for equilibrium boundary layer over land, *J. Hydrometeorol.*, *1*(6), 507–523, doi:10.1175/1525-7541(2000)001<0507:IMFEBL>2.0.CO;2.

Betts, A. K., and W. Ridgway (1989), Climatic equilibrium of the atmospheric convective boundary layer over a tropical ocean, *J. Atmos. Sci.*, *46*(17), 2621–2641, doi:10.1175/1520-0469(1989)046<2621:CEOTAC>2.0.CO;2.

Betts, A. K., et al. (2004), Coupling between CO$_2$, water vapor, temperature, and radon and their fluxes in an idealized equilibrium boundary layer over land, *J. Geophys. Res.*, *109*, D18103, doi:10.1029/2003JD004420.

Chen, B. Z., et al. (2008), Comparison of regional carbon flux estimates from CO$_2$ concentration measurements and remote sensing based footprint integration, *Global Biogeochem. Cycles*, *22*, GB2012, doi:10.1029/2007GB003024.

Ciais, P., and H. A. J. Meijer (1998), The ^{18}O/^{16}O isotope ratio of atmospheric CO$_2$ and its role in global carbon cycle research, in *Stable Isotopes*, edited by H. Griffiths, pp. 409–431, BIOS Sci. Publ., Oxford, U. K.

Conway, T. J., et al. (1994), Evidence for interannual variability of the carbon cycle from the National Oceanic and Atmospheric Administration Climate Monitoring and Diagnostics Laboratory global air sampling network, *J. Geophys. Res.*, *99*(D11), 22,831–22,855, doi:10.1029/94JD01951.

de Arellano, J. V. G., et al. (2004), Entrainment process of carbon dioxide in the atmospheric boundary layer, *J. Geophys. Res.*, *109*, D18110, doi:10.1029/2004JD004725.

Denmead, O. T., et al. (1996), Boundary layer budgets for regional estimates of scalar fluxes, *Global Change Biol.*, *2*(3), 255–264, doi:10.1111/j.1365-2486.1996.tb00077.x.

Denning, A. S. (1995), Latitudinal gradient of atmospheric CO$_2$ due to seasonal exchange with land biota, *Nature*, *376*(6537), 240–243.

Denning, A. S., et al. (1996), Simulations of terrestrial carbon metabolism and atmospheric CO$_2$ in a general circulation model. 2.Simulated CO$_2$ concentrations, *Tellus, Ser. B*, *48*(4), 543–567, doi:10.1034/j.1600-0889.1996.t01-1-00010.x.

Denning, A. S., et al. (2003), Simulated variations in atmospheric CO$_2$ over a Wisconsin forest using a coupled ecosystem-atmosphere model, *Global Change Biol.*, *9*(9), 1241–1250, doi:10.1046/j.1365-2486.2003.00613.x.

Denning, A. S., et al. (2008), Evaluation of modeled atmospheric boundary layer depth at the WLEF tower, *Agric. For. Meteorol.*, *148*(2), 206–215.

Desai, A. R., et al. (2010), Climatic controls of interannual variability in regional carbon fluxes from top-down and bottom-up perspectives, *J. Geophys. Res.*, *115*, G02011, doi:10.1029/2009JG001122.

Desjardins, R. L., et al. (1992), Aircraft-based and tower-based fluxes of carbon dioxide, latent, and sensible heat, *J. Geophys. Res.*, *97*(D17), 18,477–18,485.

Dolman, A. J., et al. (2006), The CarboEurope regional experiment strategy, *Bull. Am. Meteorol. Soc.*, *87*(10), 1367–1379, doi:10.1175/BAMS-87-10-1367.

Dolman, A. J., et al. (2009), Detecting regional variability in sources and sinks of carbon dioxide: A synthesis, *Biogeosciences*, *6*(6), 1015–1026, doi:10.5194/bg-6-1015-2009.

Enting, I. G., et al. (1995), A synthesis inversion of the concentration and δ^{13}C of atmospheric CO$_2$, *Tellus, Ser. B*, *47*(1–2), 35–52, doi:10.1034/j.1600-0889.47.issue1.5.x.

Fan, S., et al. (1998), A large terrestrial carbon sink in North America implied by atmospheric and oceanic carbon dioxide data and models, *Science*, *282*(5388), 442–446, doi:10.1126/science.282.5388.442.

Fitzjarrald, D. R. (2004), Boundary layer budgeting, in *Vegetation, Water, Humans and the Climate: A New Perspective on an Interactive System*, edited by P. C. Kabat et al., pp. 189–196, Springer, New York.

Fitzjarrald, D. R., and M. Garstang (1981), Vertical structure of the tropical boundary layer, *Mon. Weather Rev.*, *109*(7), 1512–1526, doi:10.1175/1520-0493(1981)109<1512:VSOTTB>2.0.CO;2.

Freedman, J. M., et al. (2001), Boundary layer clouds and vegetation-atmosphere feedbacks, *J. Clim.*, *14*(2), 180–197, doi:10.1175/1520-0442(2001)013<0180:BLCAVA>2.0.CO;2.

Gamon, J. A., et al. (2006a), A mobile tram system for systematic sampling of ecosystem optical properties, *Remote Sens. Environ.*, *103*(3), 246–254, doi:10.1016/j.rse.2006.04.006.

Gamon, J. A., et al. (2006b), Spectral Network (SpecNet): What is it and why do we need it?, *Remote Sens. Environ.*, *103*(3), 227–235, doi:10.1016/j.rse.2006.04.003.

Gatti, L. V., et al. (2010), Vertical profiles of CO$_2$ above eastern Amazonia suggest a net carbon flux to the atmosphere and balanced biosphere between 2000 and 2009, *Tellus, Ser. B*, *62*(5), 581–594, doi:10.1111/j.1600-0889.2010.00484.x.

Gerbig, C., et al. (2003), Toward constraining regional-scale fluxes of CO$_2$ with atmospheric observations over a continent: 2. Analysis of COBRA data using a receptor-oriented framework, *J. Geophys. Res.*, *108*(D24), 4757, doi:10.1029/2003JD003770.

Gibert, F., et al. (2007), Retrieval of average CO$_2$ fluxes by combining in situ CO$_2$ measurements and backscatter lidar information, *J. Geophys. Res.*, *112*, D10301, doi:10.1029/2006JD008190.

Gioli, B., et al. (2004), Comparison between tower and aircraft-based eddy covariance fluxes in five European regions, *Agric. For. Meteorol.*, *127*(1–2), 1–16, doi:10.1016/j.agrformet.2004.08.004.

GLOBALVIEW-CO2 (2009), *Cooperative Atmospheric Data Integration Project: Carbon Dioxide* [CD-ROM], NOAA ESRL, Boulder, Colo. (Also available on Internet via anonymous FTP to ftp.cmdl.noaa.gov, Path: Ccg/co2/GLOBALVIEW).

Gloor, M., et al. (2001), What is the concentration footprint of a tall tower?, *J. Geophys. Res.*, *106*(D16), 17,831–17,840, doi:10.1029/2001JD900021.

Goulden, M. L., et al. (1996), Measurements of carbon sequestration by long-term eddy covariance: Methods and a critical evaluation of accuracy, *Global Change Biol.*, *2*(3), 169–182, doi:10.1111/j.1365-2486.1996.tb00070.x.

Gurney, K. R., et al. (2002), Towards robust regional estimates of CO$_2$ sources and sinks using atmospheric transport models, *Nature*, *415*(6872), 626–630, doi:10.1038/415626a.

Gurney, K. R., et al. (2003), TransCom 3 CO2 inversion intercomparison: 1. Annual mean control results and sensitivity to transport and prior flux information, *Tellus Ser. B*, *55*(2), 555–579.

Helliker, B. R., et al. (2004), Estimates of net CO$_2$ flux by application of equilibrium boundary layer concepts to CO$_2$ and water vapor measurements from a tall tower, *J. Geophys. Res.*, *109*, D20106, doi:10.1029/2004JD004532.

Helliker, B. R., et al. (2005), Regional-scale estimates of forest CO$_2$ and isotope flux based on monthly CO$_2$ budgets of the atmospheric boundary layer, in *The Carbon Balance of Forest Biomes*, edited by H. Griffiths and P. G. Jarvis, pp. 77–92, Taylor and Francis, New York.

Hollinger, D. Y., et al. (2004), Spatial and temporal variability in forest-atmosphere CO$_2$ exchange, *Global Change Biol.*, *10*(10), 1689–1706, doi:10.1111/j.1365-2486.2004.00847.x.

Holzworth, G. (Ed.) (1972), Mixing Heights, Wind Speeds, and Potential for Urban Air Pollution Throughout the Contiguous United States, Off. Air Programs Publ. AP-101, U. S. Environ. Prot. Agency, Research Triangle Park, N. C.

Hurwitz, M. D., et al. (2004), Transport of carbon dioxide in the presence of storm systems over a Northern Wisconsin forest, *J. Atmos. Sci.*, *61*(5), 607–618, doi:10.1175/1520-0469(2004)061<0607:TOCDIT>2.0.CO;2.

Kalnay, E., et al. (1996), The NCEP/NCAR 40-year reanalysis project, *Bull. Am. Meteorol. Soc.*, *77*, 437–470.

Katul, G., et al. (2001), Multiscale analysis of vegetation surface fluxes: From seconds to years, *Adv. Water Resour.*, *24*(9–10), 1119–1132.

Keeling, C. D., et al. (1996), Increased activity of northern vegetation inferred from atmospheric CO$_2$ measurements, *Nature*, *382*(6587), 146–149, doi:10.1038/382146a0.

Keeling, C. D., S. C. Piper, T. P. Whorf, and R. F. Keeling (2011), Evolution of natural and anthropogenic fluxes of atmospheric CO$_2$ from 1957 to 2003, *Tellus, Ser. B*, *63*, 1–22.

Kim, J., and S. B. Verma (1991), Modeling canopy stomatal conductance in a temperate grassland ecosystem, *Agric. For. Meteorol.*, *55*(1–2), 149–166, doi:10.1016/0168-1923(91)90028-O.

Knapp, A. K. (1984), Water relations and growth of 3 grasses during wet and drought years in a tallgrass prairie, *Oecologia*, *65*(1), 35–43, doi:10.1007/BF00384460.

Lai, C. T., et al. (2003), Isotopic air sampling in a tallgrass prairie to partition net ecosystem CO$_2$ exchange, *J. Geophys. Res.*, *108*(D18), 4566, doi:10.1029/2002JD003369.

Lai, C. T., et al. (2004), Estimating photosynthetic ^{13}C discrimination in terrestrial CO$_2$ exchange from canopy to regional scales, *Global Biogeochem. Cycles*, *18*, GB1041, doi:10.1029/2003GB002148.

Lai, C. T., et al. (2005), Canopy-scale δ^{13}C of photosynthetic and respiratory CO$_2$ fluxes: Observations in forest biomes across the United States, *Global Change Biol.*, *11*(4), 633–643, doi:10.1111/j.1365-2486.2005.00931.x.

Lai, C. T., et al. (2006a), Regional CO$_2$ fluxes inferred from mixing ratio measurements: Estimates from flask air samples in central Kansas, USA, *Tellus, Ser. B*, *58*(5), 523–536, doi:10.1111/j.1600-0889.2006.00203.x.

Lai, C. T., et al. (2006b), Seasonal and interannual variations of carbon and oxygen isotopes of respired CO$_2$ in a tallgrass prairie: Measurements and modeling results from 3 years with contrasting water availability, *J. Geophys. Res.*, *111*, D08S06, doi:10.1029/2005JD006436.

Larson, V. E., and H. Volkmer (2008), An idealized model of the one-dimensional carbon dioxide rectifier effect, *Tellus, Ser. B*, *60*(4), 525–536, doi:10.1111/j.1600-0889.2008.00368.x.

Law, R. M., and P. J. Rayner (1999), Impacts of seasonal covariance on CO2 inversions, *Global Biogeochem. Cycles*, *13*(4), 845–856.

Le Quéré, C., et al. (2009), Trends in the sources and sinks of carbon dioxide, *Nat. Geosci.*, *2*(12), 831–836, doi:10.1038/ngeo689.

Levy, P. E., et al. (1999), Regional-scale CO$_2$ fluxes over central Sweden by a boundary layer budget method, *Agric. For. Meteorol.*, *99*, 169–180, doi:10.1016/S0168-1923(99)00096-9.

Lloyd, J., et al. (2001), Vertical profiles, boundary layer budgets, and regional flux estimates for CO$_2$ and its ^{13}C/^{12}C ratio and for water vapor above a forest/bog mosaic in central Siberia, *Global Biogeochem. Cycles*, *15*(2), 267–284, doi:10.1029/1999GB001211.

Mahecha, M. D., et al. (2010), Comparing observations and process-based simulations of biosphere-atmosphere exchanges on multiple timescales, *J. Geophys. Res.*, *115*, G02003, doi:10.1029/2009JG001016.

Mahrt, L. (1998), Flux sampling errors for aircraft and towers, *J. Atmos. Oceanic Technol.*, 15(2), 416–429, doi:10.1175/1520-0426(1998) 015<0416:FSEFAA>2.0.CO;2.

Masarie, K. A., and P. P. Tans (1995), Extension and integration of atmospheric carbon dioxide data into a globally consistent measurement record, *J. Geophys. Res.*, 100(D6), 11,593–11,610, doi:10.1029/ 95JD00859.

McNaughton, K. G. (1989), Regional interactions between canopies and the atmosphere, in *Plant Canopies: Their Growth, Form and Function, Soc. for Exp. Biol. Seminar Ser.*, vol. 31, edited by G. Russell, B. Marshall, and P. G. Jarvis, pp. 63–82, Cambridge Univ. Press, Cambridge, U. K., doi:10.1017/CBO9780511752308.005.

Melgarejo, J. W., and J. W. Deardorff (1974), Stability function for the boundary layer resistance laws based upon observed boundary layer heights, *J. Atmos. Sci.*, 31, 1324–1353, doi:10.1175/1520-0469(1974) 031<1324:SFFTBL>2.0.CO;2.

Moffat, A. M., et al. (2007), Comprehensive comparison of gap-filling techniques for eddy covariance net carbon fluxes, *Agric. For. Meteorol.*, 147(3–4), 209–232.

Moore, K. E., and D. R. Fitzjarrald (1993), How well can regional fluxes be derived from smaller-scale estimates, *J. Geophys. Res.*, 98(D4), 7187–7198, doi:10.1029/93JD00029.

Papale, D., et al. (2006), Towards a standardized processing of Net Ecosystem Exchange measured with eddy covariance technique: algorithms and uncertainty estimation, *Biogeosciences*, 3(4), 571–583.

Paw, U. K. T., et al. (2004), Carbon dioxide exchange between an old-growth forest and the atmosphere, *Ecosystems*, 7(5), 513–524.

Peters, W., et al. (2007), An atmospheric perspective on North American carbon dioxide exchange: CarbonTracker, *Proc. Natl. Acad. Sci. U. S. A.*, 104(48), 18,925–18,930, doi:10.1073/pnas.0708986104.

Priestley, C. H. B., and R. J. Taylor (1972), On the assessment of surface heat flux and evaporation using large-scale parameters, *Monthly Weather Rev.*, 100(2), 81–92.

Raupach, M. R. (1991), Vegetation-atmosphere interaction in homogenous and heterogeneous terrain: Some implications of mixed-layer dynamics, *Vegetatio*, 91(1–2), 105–120, doi:10.1007/BF00036051.

Raupach, M. R. (2000), Equilibrium evaporation and the convective boundary layer, *Boundary Layer Meteorol.*, 96(1–2), 107–141.

Raupach, M. R., et al. (2005), Model-data synthesis in terrestrial carbon observation: Methods, data requirements and data uncertainty specifications, *Global Change Biol.*, 11(3), 378–397, doi:10.1111/j.1365-2486. 2005.00917.x.

Rayner, P. J., and D. M. O'Brien (2001), The utility of remotely sensed CO₂ concentration data in surface source inversions, *Geophys. Res. Lett.*, 28(1), 175–178, doi:10.1029/2000GL011912.

Reichstein, M., et al. (2005), On the separation of net ecosystem exchange into assimilation and ecosystem respiration: review and improved algorithm, *Global Change Biol.*, 11(9), 1424–1439.

Running, S. W., et al. (2004), A continuous satellite-derived measure of global terrestrial primary production, *BioScience*, 54(6), 547–560, doi:10.1641/0006-3568(2004)054[0547:ACSMOG]2.0.CO;2.

Schauer, A. J., et al. (2003), An automated sampler for collection of atmospheric trace gas samples for stable isotope analyses, *Agric. For. Meteorol.*, 118(1–2), 113–124, doi:10.1016/S0168-1923(03)00065-0.

Schauer, A. J., et al. (2005), An automated system for stable isotope and concentration analyses of CO₂ from small atmospheric samples, *Rapid Commun. Mass Spectrom.*, 19(3), 359–362, doi:10.1002/rcm.1792.

Stephens, B. B., et al. (2007), Weak northern and strong tropical land carbon uptake from vertical profiles of atmospheric CO₂, *Science*, 316(5832), 1732–1735, doi:10.1126/science.1137004.

Stull, R. B. (Ed.) (1988), *An Introduction to Boundary Layer Meteorology*, 666 pp., Springer, New York.

Styles, J. M., et al. (2002), Estimates of regional surface carbon dioxide exchange and carbon and oxygen isotope discrimination during photosynthesis from concentration profiles in the atmospheric boundary layer, *Tellus, Ser. B*, 54(5), 768–783, doi:10.1034/j.1600-0889.2002.01336.x.

Sun, J. L., et al. (2010), A multiscale and multidisciplinary investigation of ecosystem-atmosphere CO₂ exchange over the rocky mountains of Colorado, *Bull. Am. Meteorol. Soc.*, 91(2), 209–230, doi:10.1175/ 2009BAMS2733.1.

Tans, P. P., et al. (1990), Observational constraints on the global atmospheric CO₂ budget, *Science*, 247(4949), 1431–1438, doi:10.1126/ science.247.4949.1431.

Teixeira, J., et al. (2008), Parameterization of the atmospheric boundary layer, *Bull. Am. Meteorol. Soc.*, 89(4), 453–458.

Thoning, K. W., et al. (1989), Atmospheric carbon dioxide at Mauna Loa observatory 2.analysis of the NOAA GMCC data, 1974–1985, *J. Geophys. Res.*, 94(D6), 8549–8565, doi:10.1029/JD094iD06p08549.

Urbanski, S., et al. (2007), Factors controlling CO₂ exchange on timescales from hourly to decadal at Harvard Forest, *J. Geophys. Res.*, 112, G02020, doi:10.1029/2006JG000293.

van Heerwaarden, C. C., et al. (2009), Interactions between dry-air entrainment, surface evaporation and convective boundary-layer development, *Q. J. R. Meteorol. Soc.*, 135(642), 1277–1291.

Wang, J. W., et al. (2007), Observations and simulations of synoptic, regional, and local variations in atmospheric CO₂, *J. Geophys. Res.*, 112, D10308, doi:10.1029/2006JD007770.

Wang, Y. P., et al. (2009), A review of applications of model-data fusion to studies of terrestrial carbon fluxes at different scales, *Agric. For. Meteorol.*, 149(11), 1829–1842.

Wofsy, S. C., et al. (1988), Carbon dioxide in the atmosphere over the amazon basin, *J. Geophys. Res.*, 93(D2), 1377–1387, doi:10.1029/ JD093iD02p01377.

Xiao, J. F., et al. (2008), Estimation of net ecosystem carbon exchange for the conterminous United States by combining MODIS and Ameri-Flux data, *Agric. For. Meteorol.*, 148(11), 1827–1847, doi:10.1016/j. agrformet.2008.06.015.

Xiao, J. F., et al. (2010), A continuous measure of gross primary production for the conterminous United States derived from MODIS and AmeriFlux data, *Remote Sens. Environ.*, 114(3), 576–591, doi:10.1016/j.rse.2009. 10.013.

Xiao, J. F., et al. (2011), Assessing net ecosystem carbon exchange of US terrestrial ecosystems by integrating eddy covariance flux measurements and satellite observations, *Agric. For. Meteorol.*, 151(1), 60–69, doi:10.1016/j.agrformet.2010.09.002.

Yi, C., et al. (2000), Influence of advection on measurements of the net ecosystem-atmosphere exchange of CO₂ from a very tall tower, *J. Geophys. Res.*, 105(D8), 9991–9999, doi:10.1029/2000JD900080.

Yi, C., et al. (2001), Long-term observations of the dynamics of the continental planetary boundary layer, *J. Atmos. Sci.*, 58, 1288–1299, doi:10.1175/1520-0469(2001)058<1288:LTOOTD>2.0.CO;2.

Yi, C., et al. (2004), Observed covariance between ecosystem carbon exchange and atmospheric boundary layer dynamics at a site in northern Wisconsin, *J. Geophys. Res.*, 109, D08302, doi:10.1029/2003JD004164.

X. Dang and C.-T. Lai, Department of Biology, San Diego State University, 5500 Campanile Dr., San Diego, CA 92182-4614, USA. (lai@sciences.sdsu.edu)

J. R. Ehleringer, Department of Biology, University of Utah, 257 S., 1400 E., Salt Lake City, UT 84112, USA.

D. Y. Hollinger, Northern Research Station, USDA Forest Service, 271 Mast Rd., Durham, NH 03824, USA.

J. W. Munger, School of Engineering and Applied Science and Department of Earth and Planetary Science, Harvard University, 20 Oxford St., Cambridge, MA 02138, USA.

C. Owensby, Department of Agronomy, Kansas State University, Manhattan, KS 66506, USA.

A. J. Schauer, Department of Earth and Space Sciences, University of Washington, Seattle, WA 84112-0840, USA.

J. Xiao, Complex Systems Research Center, Institute for the Study of Earth, Oceans, and Space, University of New Hampshire, 8 College Rd., Durham, NH 03861, USA.